

# Ocean acidification has different effects on the production of dimethylsulfide and dimethylsulfoniopropionate measured in cultures of *Emiliana huxleyi* and a mesocosm study: a comparison of laboratory monocultures and community interactions

Alison L. Webb,<sup>A,F</sup> Gill Malin,<sup>A</sup> Frances E. Hopkins,<sup>B</sup> Kai Lam Ho,<sup>A</sup> Ulf Riebesell,<sup>C</sup> Kai G. Schulz,<sup>C,E</sup> Aud Larsen<sup>D</sup> and Peter S. Liss<sup>A</sup>

<sup>A</sup>Centre for Ocean and Atmospheric Sciences, School of Environmental Sciences, University of East Anglia, Norwich Research Park, Norwich, NR4 7TJ, UK.

<sup>B</sup>Plymouth Marine Laboratory, Prospect Place, Plymouth, Devon PL1 3DH, UK.

<sup>C</sup>GEOMAR Helmholtz Centre for Ocean Research Kiel, Düsternbrooker Weg 20, D-24148 Kiel, Germany.

<sup>D</sup>Uni Research Environment, Thormøhlensgate 49 B, N-5006 Bergen, Norway.

<sup>E</sup>Present address: Centre for Coastal Biogeochemistry, School of Environmental Science and Management, Southern Cross University, Lismore, NSW 2480, Australia.

<sup>F</sup>Corresponding author. Present address: Groningen Institute for Evolutionary Life Sciences, University of Groningen, PO Box 1110, NL-9700 CC Groningen, Netherlands. Email: a.l.webb@rug.nl

**Environmental context.** Approximately 25 % of CO<sub>2</sub> released to the atmosphere by human activities has been absorbed by the oceans, resulting in ocean acidification. We investigate the acidification effects on marine phytoplankton and subsequent production of the trace gas dimethylsulfide, a major route for sulfur transfer from the oceans to the atmosphere. Increasing surface water CO<sub>2</sub> partial pressure (*p*CO<sub>2</sub>) affects the growth of phytoplankton groups to different degrees, resulting in varying responses in community production of dimethylsulfide.

**Abstract.** The human-induced rise in atmospheric carbon dioxide since the industrial revolution has led to increasing oceanic carbon uptake and changes in seawater carbonate chemistry, resulting in lowering of surface water pH. In this study we investigated the effect of increasing CO<sub>2</sub> partial pressure (*p*CO<sub>2</sub>) on concentrations of volatile biogenic dimethylsulfide (DMS) and its precursor dimethylsulfoniopropionate (DMSP), through monoculture studies and community *p*CO<sub>2</sub> perturbation. DMS is a climatically important gas produced by many marine algae: it transfers sulfur into the atmosphere and is a major influence on biogeochemical climate regulation through breakdown to sulfate and formation of subsequent cloud condensation nuclei (CCN). Overall, production of DMS and DMSP by the coccolithophore *Emiliana huxleyi* strain RCC1229 was unaffected by growth at 900  $\mu$ atm *p*CO<sub>2</sub>, but DMSP production normalised to cell volume was 12 % lower at the higher *p*CO<sub>2</sub> treatment. These cultures were compared with community DMS and DMSP production during an elevated *p*CO<sub>2</sub> mesocosm experiment with the aim of studying *E. huxleyi* in the natural environment. Results contrasted with the culture experiments and showed reductions in community DMS and DMSP concentrations of up to 60 and 32 % respectively at *p*CO<sub>2</sub> up to 3000  $\mu$ atm, with changes attributed to poorer growth of DMSP-producing nanophytoplankton species, including *E. huxleyi*, and potentially increased microbial consumption of DMS and dissolved DMSP at higher *p*CO<sub>2</sub>. DMS and DMSP production differences between culture and community likely arise from pH affecting the inter-species responses between microbial producers and consumers.

Received 16 December 2014, accepted 13 July 2015, published online 26 October 2015

## Introduction

Since the 1750s, atmospheric carbon dioxide concentrations have increased from 280 to close to 400  $\mu$ atm today because of anthropogenic inputs from burning fossil fuels, cement production and land use changes.<sup>[1]</sup> The atmospheric CO<sub>2</sub> concentrations projected for 2100 are in the range 350–840  $\mu$ atm; the majority of climate change scenarios project continuing

increases over coming decades, with the possibility of decline through immediate change to low-carbon economies.<sup>[2]</sup> Approximately 25 % of the total CO<sub>2</sub> emitted into the atmosphere by anthropogenic activities has been absorbed into the oceans to date, making the oceans a crucial sink for CO<sub>2</sub>, with other sinks including the atmosphere (~45 %) and land-based vegetation (~30 %).<sup>[3]</sup> Dissolution of CO<sub>2</sub> in seawater results in

the formation of carbonic acid, which readily dissociates to release  $H^+$  and lowers the pH, an effect termed ‘ocean acidification’. Surface ocean pH levels will very likely be up to 0.4 units lower by 2100, a concomitant 150% increase in  $H^+$  ions, which will decrease the carbonate saturation state and result in increasing dissolution of calcium carbonate in surface waters.<sup>[4,5]</sup>

*Emiliana huxleyi* is a globally distributed haptophyte which produces calcite plates (coccoliths) covering the cell surface. Large-scale blooms of *E. huxleyi* occur in temperate shelf seas, including the North West European continental shelf in early summer,<sup>[6]</sup> and total global production of calcite by *E. huxleyi* makes it the most productive calcifying organism on Earth.<sup>[7]</sup> Under conditions of elevated  $CO_2$  partial pressure ( $pCO_2$ ) in an ocean acidification scenario, calcite production by *E. huxleyi* has been found to typically decrease.<sup>[8,9]</sup> Calcium carbonate formation is a reaction that liberates  $CO_2$  ( $Ca^{2+} + 2HCO_3^- \rightarrow CaCO_3 + CO_2 + H_2O$ ), and any reduction in calcification rate can act as a negative feedback on rising surface water  $pCO_2$ .<sup>[10]</sup> Over longer timescales, calcite and organic carbon production by calcifying phytoplankton, and subsequent post-bloom settlement of this material through the water column is a major route for carbon transport from the surface oceans to storage in deeper waters.<sup>[11]</sup> Decreased surface pH could affect growth and subsequent calcite production and carbon fixation by *E. huxleyi* and have a significant effect on global cycling and removal of carbon in the future ocean.<sup>[8]</sup>

*E. huxleyi* is also a significant producer of dimethylsulfoniopropionate (DMSP), a compound produced by many phytoplankton species for several suggested purposes: as an osmoregulatory compound,<sup>[12]</sup> cryoprotectant,<sup>[13]</sup> antioxidant,<sup>[14]</sup> grazing defence<sup>[15]</sup> or chemoattractant.<sup>[16,17]</sup> DMSP is recognised as a significant part of the sulfur and carbon fluxes through marine microbial food webs, providing a reported 0.5 to 6% of total carbon demand and between 3 and 100% of total sulfur demand by marine bacteria<sup>[18]</sup> and major phytoplankton groups.<sup>[19]</sup> Breakdown of DMSP is a significant source of dimethylsulfide (DMS), a volatile compound released through the surface microlayer to the atmosphere where it oxidises to form sulfate-containing particles. These particles can act as cloud condensation nuclei (CCN) in the troposphere, where cloud formation can reflect the Sun’s energy back into space, with implications for global climate regulation.<sup>[20,21]</sup> The marine DMS-associated global sulfur flux to the atmosphere has been calculated at  $28.1 \text{ Tg S year}^{-1}$ .<sup>[22]</sup>

Previous community  $pCO_2$  perturbation (mesocosm) experiments in natural waters have identified changes in DMS and DMSP concentrations as  $pCO_2$  increased.<sup>[23–28]</sup> Here we investigated the effects of elevated  $pCO_2$  on DMS and DMSP production in a low-bacterial abundance monoculture of *E. huxleyi* (strain RCC1229), and progressed to investigate the effect of  $pCO_2$  on a community known to contain a natural *E. huxleyi* population. The hypotheses of this investigation were that elevated  $pCO_2$  would affect the physiology of the *E. huxleyi* cell and result in lower production of intracellular DMSP, which would result in lower DMS production. On a community level, elevated  $pCO_2$  may stimulate primary productivity, resulting in increased community DMSP synthesis and higher DMSP concentrations.<sup>[29]</sup> In contrast, an increase in bacterial productivity at elevated  $pCO_2$  would create a greater demand for sulfur and increase DMS and DMSP consumption.<sup>[30,31]</sup> This investigation aimed to determine if changes in DMS and DMSP concentrations under high  $pCO_2$  are a result of physiological changes in

the *E. huxleyi* cell, or changes in microbial inter-species responses to elevated  $pCO_2$ , nutrient competition and DMSP consumption.

### *Emiliana huxleyi* culture setup

*E. huxleyi* strain RCC1229 was chosen for its high level of calcification and origin in the North Sea (as a strain isolated close to the location of the mesocosm experiment) and grown in autoclaved aged natural seawater medium enriched with ESAW (Enriched Seawater Artificial Water) nutrients (starting concentration  $186.7 \mu\text{mol L}^{-1} \text{NO}_3$  and  $20.1 \mu\text{mol L}^{-1} \text{PO}_4$ ) and vitamins.<sup>[32]</sup> The stock culture was treated for 2 days with a broad-spectrum antibiotic mixture<sup>[33]</sup> to significantly reduce bacterial abundance, before regular reinoculation into fresh medium to maintain exponential growth for 10 days before  $pCO_2$  perturbation (day T0). All cultures were maintained at  $15^\circ\text{C}$  in a 16:8 light–dark cycle with light at  $180 \mu\text{mol photons m}^{-2} \text{s}^{-1}$ .

Cells were grown in a semicontinuous culture, with three replicate cultures exposed to  $900 \mu\text{atm } pCO_2$  and three replicate control cultures treated with air at ambient  $pCO_2$  ( $395 \mu\text{atm}$ ). Prior to inoculation, the medium was filter sterilised, decanted into two bespoke vessels and pre-sparged to the  $pCO_2$  treatment concentration using pre-prepared  $CO_2$  gas mixtures (BOC Ltd, UK). Cultures were grown in 1-L Erlenmeyer flasks with 500 mL of pre-prepared sterile medium and sufficient inoculum to provide a starting cell count of  $120\,000 \text{ cells mL}^{-1}$ . Cultures were grown over 4-day periods to cell densities of  $\sim 1\,000\,000 \text{ cells mL}^{-1}$  before re-inoculation into fresh medium to keep the culture in exponential growth. Flasks were sealed with ground glass Quikfit stoppers modified to enable inlet and outlet gas lines. Aqueous phase bubbling of the cultures was avoided but the headspaces of each flask were flushed daily with the respective treatment gas for 10 min at a rate of  $30 \text{ mL min}^{-1}$  through a  $0.2\text{-}\mu\text{m}$  Minisart filter (Sartorius Ltd, Epsom, UK). Samples were extracted from the flasks through a luer-lock sealed opening in the base of the flask; to prevent contamination of the culture, all sampling from this outlet used sterile luer fittings on 25-mL glass syringes.

### Measurement of biological parameters

Culture samples for cell volume (CV), cell counts, pH, DMS and total DMSP (DMSP<sub>T</sub>) were taken daily 7 h after the onset of the light period. CV and counts were measured in triplicate from live culture using a Coulter Multisizer III (Beckman Coulter Ltd, High Wycombe, UK). Average growth rates were determined for each inoculation period as  $\ln(N_1/N_0)/(t_1 - t_0)$ , with cell counts  $N_0$  and  $N_1$  taken at the time points  $t_0$  and  $t_1$  respectively. All six cultures were examined under  $100\times$  magnification using an Olympus BX40F-3 fluorescence microscope and no non-calcified cells could be identified from multiple prepared samples. For pH analysis, 20 mL of culture from each flask was analysed daily at  $15^\circ\text{C}$  by the standard potentiometric technique<sup>[34,35]</sup> using a Seven Easy S20 probe with automatic temperature adjustment (relative accuracy  $\pm 0.01$  Mettler–Toledo Ltd, Beaumont Leys, UK) using National Bureau of Standards (NBS) buffers.

### DMS and DMSP analysis

DMS samples were extracted by injection of 2 mL of filtered culture into a polytetrafluoroethylene (PTFE) purge and cryo-trap system and purged with oxygen-free nitrogen (OFN) for

5 min at 80 mL min<sup>-1</sup>. Samples were trapped in a PTFE sample loop suspended above liquid nitrogen and held at -150 °C, before immersion in boiling water and injection into a Shimadzu GC2010 gas chromatograph (GC) with a Varian Chrompack CP-Sil-5CB column (30 m, 0.53-mm internal diameter (ID)) and flame photometric detector (FPD). The GC was operated isothermally at 60 °C and DMS eluted at 2.1 min; the GC was calibrated using liquid DMSP standards treated with 10 M NaOH in the concentration range 5.07–406.2 nmol L<sup>-1</sup> (7 % analytical error through analysis of 10 samples). Six-point calibrations were performed weekly and checked daily for instrument drift, and the resulting calibrations typically produced linear regression with  $r^2 > 0.99$ . The same method was used when participating in the AQA 12–23 international DMS analysis proficiency test in February 2013 and achieved close agreement with the known concentration of the test material.<sup>[36]</sup>

Triplicate DMSP<sub>T</sub> samples from each flask were prepared in 4-mL headspace vials by the addition of 0.5 mL of 1 M NaOH to 3 mL of culture and sealed using PTFE screw caps and PTFE–silicone septa. All DMSP vials were stored for 24 h at 30 °C before an MPS2 Twister multi-purpose autosampler (Gerstel, Mülheim, Germany) equipped with a 250- $\mu$ L Hamilton syringe sampled 100  $\mu$ L of headspace from each vial and injected it into the GC-FPD as set up above.

### Mesocosm experiment setup

The experiment was performed at the Marine Biological Station at Espeegrend, University of Bergen, Norway from 6 May to 12 June 2011, with nine cylindrical thermoplastic polyurethane (TPU) mesocosm enclosures (~75 m<sup>3</sup>, 25-m water depth) anchored ~100 m apart and 1 mile offshore in the Raunefjord (60.265°N, 5.205°E) at a water depth of 55 to 65 m. Each enclosure was supported by an 8-m tall floating frame and capped with a polyvinyl chloride (PVC) hood.<sup>[37]</sup> Over 95 % of the incoming photosynthetically active radiation (PAR) was transmitted by the TPU and PVC materials, with near 100 % absorbance of incoming UV radiation. The mesocosms were filled on 1 May 2011 (day T-7) by lowering the bags through the CO<sub>2</sub> under-saturated post-bloom water column with the bottom openings covered with 3-mm mesh to exclude larger organisms. Full exclusion of the mesocosms from the surrounding waters occurred 3 days later: the lower opening was fitted with a sediment trap and the upper openings were raised above the water surface.<sup>[37]</sup>

The carbonate chemistry of the water was altered by the addition of CO<sub>2</sub>-saturated, filtered fjord water to alter the dissolved inorganic carbon (DIC) concentrations while keeping alkalinity constant.<sup>[38]</sup> This water was added to seven mesocosms depending on the target *p*CO<sub>2</sub> concentrations over a 5-day period, starting on 8 May 2011 (day T0). This was done with a bespoke dispersal apparatus ('Spider') that was lowered through the bags to ensure even distribution of CO<sub>2</sub>-rich waters throughout the water column. Two mesocosms were designated controls and received no addition of CO<sub>2</sub>-enriched water (M2 and M4, 280  $\mu$ atm). The range of target *p*CO<sub>2</sub> was 390 to 3000  $\mu$ atm across the seven enriched mesocosms (M6, 390  $\mu$ atm; M8, 560  $\mu$ atm; M1, 840  $\mu$ atm; M3, 1120  $\mu$ atm; M5, 1400  $\mu$ atm; M7, 2000  $\mu$ atm; M9, 3000  $\mu$ atm) taking into account IPCC projections up to the year 2300 and beyond,<sup>[2]</sup> in order to identify the change in different parameters to increasing *p*CO<sub>2</sub>. *p*CO<sub>2</sub> and pH were calculated from the coulometric measurement of DIC<sup>[39]</sup> and spectrophotometric determination

of pH<sup>[40]</sup> using the stoichiometric equilibrium constants for carbonic acid.<sup>[41,42]</sup> No further perturbation was made to the carbonate system once the experiment had commenced. Inorganic nutrients were added to each mesocosm on T14 to stimulate phytoplankton growth. The inside of the mesocosm walls was cleaned regularly with a ring-shaped, double-bladed wiper to prevent biofilm growth.<sup>[37]</sup> After termination of the experiment, one small hole was detected in the bag of M2 which had led to non-quantifiable water exchange, so the results from this mesocosm were removed from the analysis.

### DMS and DMSP extraction and analysis

An integrated water sampler (IWS, Hydrobios GmbH, Kiel, Germany) was used every morning to collect samples from the full 25-m water depth of all nine mesocosms. Samples for DMS and DMSP analysis were collected in an amber bottle from the laminar flow of the IWS using Tygon tubing and the bottle was allowed to overflow for twice the volume before the tube was removed and the glass stopper firmly inserted to prevent air bubbles and atmospheric contact. DMS samples (40 mL) were injected into a purge and cryotrap system<sup>[43]</sup> through a 25-mm Whatman GF/F (GE Healthcare Life Sciences, Little Chalfont, England) and were purged with oxygen-free nitrogen (OFN) at 80 mL min<sup>-1</sup> for 10 min. Gas samples passed through a glass wool trap, to remove aerosols and water droplets, and a series of two nafion counterflow driers operating at 180 mL min<sup>-1</sup>, before DMS was trapped in a stainless steel sample loop held above liquid nitrogen at -150 °C.

DMS samples were injected into an Agilent 6890 gas chromatograph equipped with a 60-m DB-VRX capillary column (0.32-mm ID, 1.8- $\mu$ m film thickness, Agilent J&W Ltd) according to the programme outlined by Hopkins et al.<sup>[24]</sup> Analysis was by an Agilent 5973 quadrupole mass spectrometer operated in electron ionisation (EI), single ion mode (SIM), and was calibrated using a gravimetrically prepared liquid DMS standard diluted in high performance liquid chromatography (HPLC)-grade methanol to the required concentration in the range 0.04–7.64 nmol L<sup>-1</sup> (10 % analytical error for triplicate measurements). Gas chromatography–mass spectrometry (GC-MS) instrument drift was corrected using 2  $\mu$ L of diluted deuterated DMS (D<sub>6</sub>-DMS) as a surrogate analyte.<sup>[44,45]</sup> Five-point calibrations were performed weekly, and checked daily, and the linear regression from the calibrations typically produced values of  $r^2 > 0.98$ .

DMSP<sub>T</sub> samples were prepared for later analysis using the acidification method of Curran et al.<sup>[46,47]</sup> by storing 7 mL of unfiltered aliquots of seawater in 8-mL glass sample vials (Labhut, Churcham, UK) with 0.35  $\mu$ L of 50 % H<sub>2</sub>SO<sub>4</sub>. All samples were stored in the dark at room temperature for 8 weeks before analysis. DMSP<sub>T</sub> was extracted by purging 2 mL of unfiltered sample with 1 mL of 10 M NaOH with OFN for 5 min at 80 mL min<sup>-1</sup>, before analysis by GC-FPD as described above.

### Additional measurements

Water samples were collected from the IWS every first or second day, and phytoplankton abundances were determined with a FacsCalibur flow cytometer (Becton Dickinson) equipped with an air-cooled laser providing 15 mW at 488 nm with standard filter set-up. The counts were obtained from fresh samples with the trigger set on red. Discrimination of *Synechococcus* spp., *Emiliania huxleyi* and autotrophic picoeukaryotes, cryptophytes and other autotrophic nanoeukaryotes was based on dot plots

of side-scatter signal (SSC) v. pigment autofluorescence (chlorophyll-*a* (Chl-*a*) and phycoerythrin).<sup>[48]</sup>

For determination of Chl-*a* concentrations, aliquots of 250–500 mL of sample from the IWS were also filtered onto GF/F and stored frozen for 24 h before homogenisation in 90 % acetone with glass beads. The mixture was centrifuged at 800g and the Chl-*a* concentrations were determined on a Turner AU-10 fluorometer.<sup>[49]</sup> Further samples were extracted in 100 % acetone and analysed by HPLC (WATERS HPLC with a Varian Microsorb-MV 100–3 C8 column),<sup>[50]</sup> with phytoplankton community composition calculated using the CHEMTAX algorithm by converting the concentrations of marker pigments into the Chl-*a* equivalents.<sup>[51,52]</sup>

### Statistical analysis

Statistical analysis was performed using *Minitab v16*. All data were checked for normality using an Anderson–Darling test before statistical analysis, and were transformed where necessary. Equal variance was confirmed using Levene's Tests. One-way analysis of variance (ANOVA) combined with Tukey's post analysis tests were used on the DMS and DMSP data to determine differences between the mesocosms at different  $p\text{CO}_2$  concentrations. Spearman's rank correlation was also used to determine the relationships between  $p\text{CO}_2$  and DMS and DMSP concentrations over the course of the experiment, as well as the relationships between different community variables and the trace gas concentrations. Two-tailed *t*-tests were used to determine differences between the control and  $\text{CO}_2$  treatments during the laboratory studies.

## *E. huxleyi* high $p\text{CO}_2$ culture experiment results

### Growth parameters

The pH within the  $\text{CO}_2$  treatment cultures started at a mean of 7.43 immediately following inoculation compared to 7.90 in the air control (Fig. 1a). As the culture grew, the pH gradually increased in all flasks, but in the  $\text{CO}_2$  treatment cultures the pH was significantly lower than for the air control ( $t = 7.68$ ,  $P < 0.01$ ), and re-inoculation reduced the pH in all cultures. The mean pH for the entire experiment was 7.72 in the  $\text{CO}_2$  treatment and 8.13 in the control. Cultures from both treatments grew exponentially for four days after inoculations 1, 2 and 3, and for five days in the fourth and fifth inoculations. Cell counts at the end of each inoculation period ranged from  $6.3 \times 10^5$  to  $1.34 \times 10^6$  cells  $\text{mL}^{-1}$ , and there was no increase in cell count with elevated  $\text{CO}_2$  (Fig. 1b), with an average specific growth rate of  $0.47 \text{ day}^{-1}$  in both treatments. CV varied in *E. huxleyi* cultures so the data are presented as total CV (Fig. 1c), and was used to calculate mean individual CV, which increased in the  $900 \mu\text{atm}$   $\text{CO}_2$  treatment as the experiment progressed (Fig. 1d). Mean CV in the control treatment was  $46.0 \pm 12.0 \mu\text{m}^3$  and in the  $\text{CO}_2$  treatment was  $53.4 \pm 13.8 \mu\text{m}^3$ , and cells showed a 20 % increase in volume during the fifth inoculation compared to the control treatment ( $t = -3.65$ ,  $P < 0.01$ ).

### DMS and DMSP dynamics

Aqueous DMS was measured daily (Fig. 2a) alongside the cell count and volume analyses, and was normalised to cell number (Fig. 2b). During the first two culture periods up to T9, DMS was in the range 6.5–65.1  $\text{nmol L}^{-1}$ , but during the following three culture periods, DMS increased sequentially to higher concentrations up to a mean of  $328.8 \pm 56.1 \text{ nmol L}^{-1}$  in the  $\text{CO}_2$  treatment and  $296.8 \pm 69.2 \text{ nmol L}^{-1}$  in the control at T23. DMS

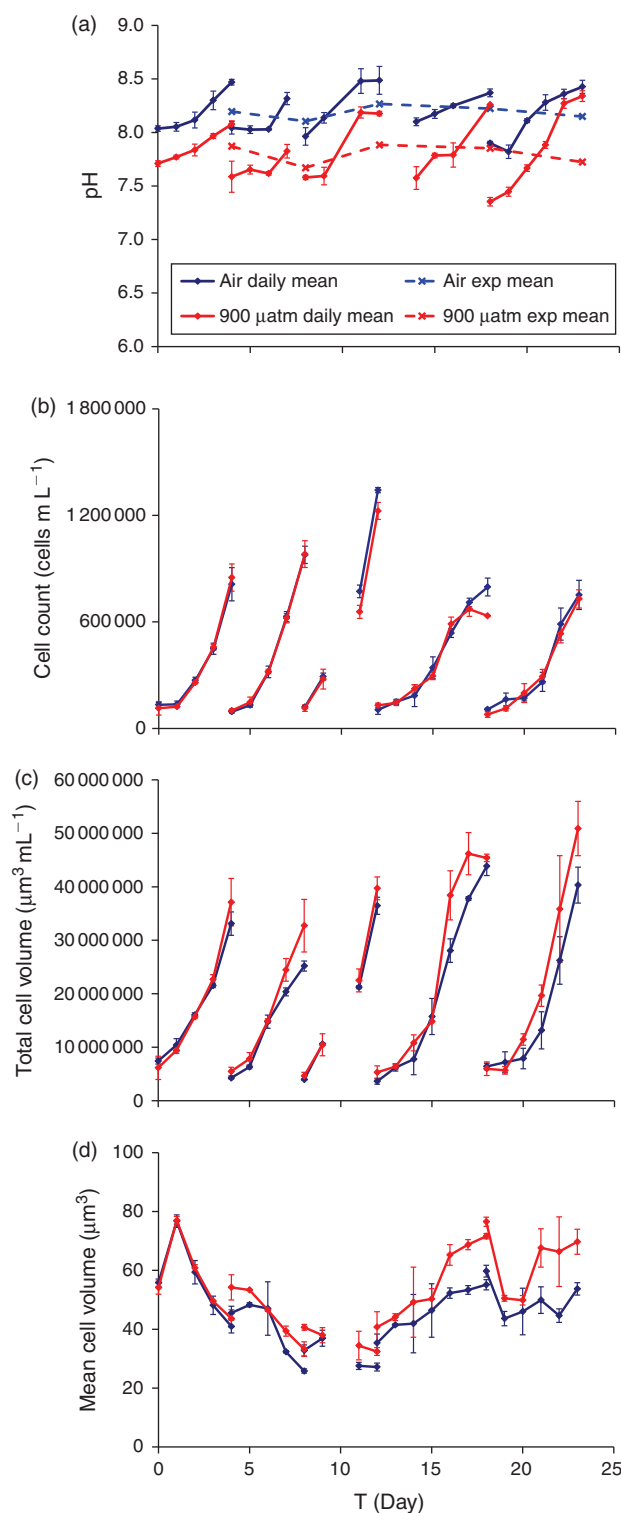


**Fig. 1.** Growth dynamics of the  $900 \mu\text{atm}$   $\text{CO}_2$  partial pressure ( $p\text{CO}_2$ ) (red) and control (blue) cultures showing the mean and standard deviation as error bars for three replicate flasks for (a) pH, (b) cell count (cells  $\text{mL}^{-1}$ ), (c) total cell volume ( $\mu\text{m}^3 \text{ mL}^{-1}$ ) and (d) individual cell volume ( $\mu\text{m}^3$ ). Dashed lines for pH show the mean pH for each inoculation period across the duration of the experiment.

data normalised to CV showed no effect of  $\text{CO}_2$  treatment on the DMS production ( $t = 0.77$ ,  $P = 0.444$ ) but was on average 80 % lower in the first inoculation compared to the final inoculation period with a range of 0.6–11.5  $\text{nmol L}^{-1}$  CV.

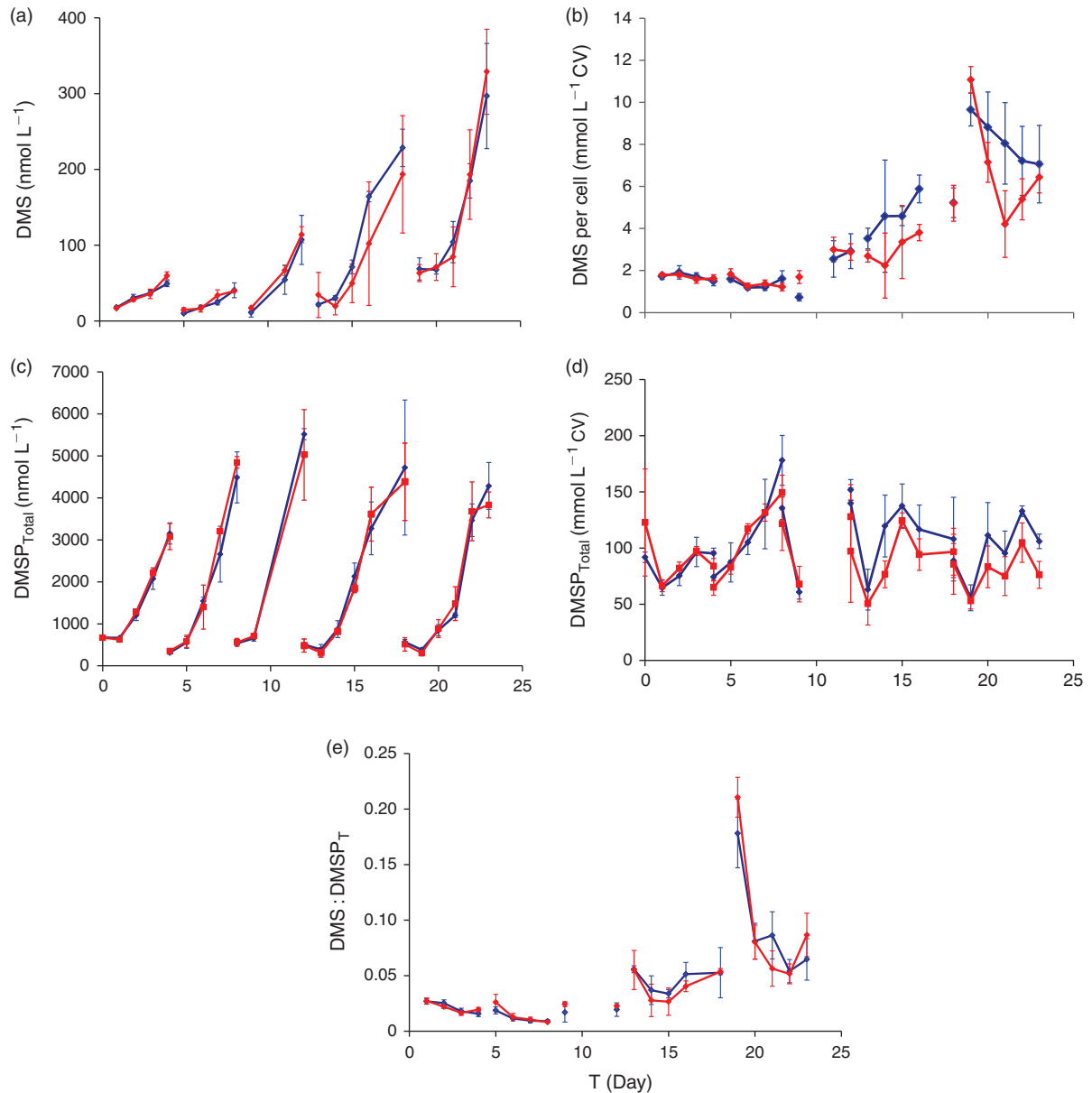


**Fig. 2.** Dimethylsulfide (DMS) and dimethylsulfoniopropionate (DMSP) dynamics of the 900  $\mu\text{atm}$   $\text{CO}_2$  partial pressure ( $p\text{CO}_2$ ) (red) and control (blue) treatments, showing the mean and standard deviation as error bars of three replicate flasks for each treatment. (a) DMS concentration ( $\text{nmol L}^{-1}$ ), (b) DMS normalised to cell volume ( $\text{mmol L}^{-1} \text{CV}$ ), (c) total  $\text{DMSP}_T$  concentration ( $\text{nmol L}^{-1}$ ), (d)  $\text{DMSP}_T$  normalised to cell volume ( $\text{mmol L}^{-1} \text{CV}$ ) and (e) DMS-to- $\text{DMSP}_T$  ratio.

$\text{DMSP}_T$  concentrations increased exponentially with cell count (Fig. 2c) from a mean of  $505.3 \pm 118.7 \text{ nmol L}^{-1}$  (control) and  $504.9 \pm 140.2 \text{ nmol L}^{-1}$  ( $\text{CO}_2$ ) in the initial days of inoculation to  $4444.5 \pm 1127.2 \text{ nmol L}^{-1}$  (control) and  $4180.2 \pm 1000.0 \text{ nmol L}^{-1}$  ( $\text{CO}_2$ ) on the final day of each inoculation.  $\text{DMSP}_T$  normalised to CV varied over the course of the experiment, within the range 16.7–202.1  $\text{mmol L}^{-1} \text{CV}$  and was 12% lower in the  $\text{CO}_2$  treatment than the control over the entire experiment (Fig. 2d;  $t = 3.71$ ,  $P < 0.01$ ,  $n = 138$ ). The measured DMS-to- $\text{DMSP}_T$  ratio was calculated (Fig. 2e) with a mean of 0.04. The ratio had a sharp peak on T19 in both treatments, reaching a maximum of 0.23 in the  $\text{CO}_2$  treatment, but over the course of the experiment, increased  $p\text{CO}_2$  had no significant effect on the DMS-to- $\text{DMSP}_T$  ratio. A summary of the *E. huxleyi* culture results is given in Table 1.

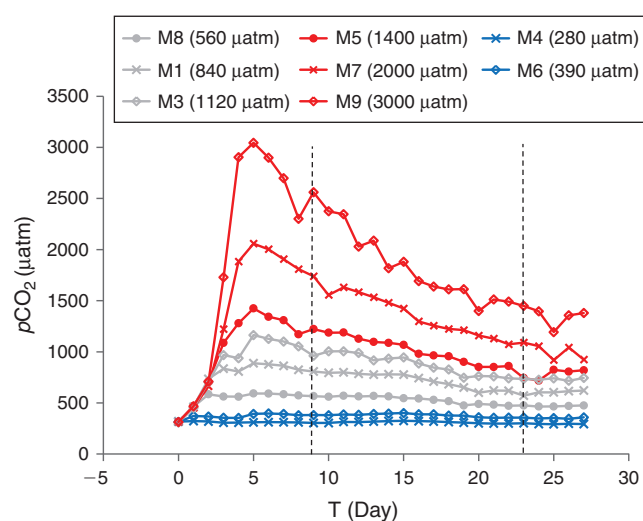
## Mesocosm experiment results

### Changes in physical oceanographic conditions

Inorganic nitrate and phosphate concentrations in the mesocosms were measured at  $1.54 \pm 0.30$  and  $0.21 \pm 0.01 \mu\text{mol L}^{-1}$  respectively on T1 of the experiment, with addition of artificial inorganic nutrients to all mesocosms on T14 to stimulate phytoplankton growth (mean concentrations  $5.0 \pm 0.2 \mu\text{mol L}^{-1}$   $\text{NO}_3$  and  $0.16 \pm 0.02 \mu\text{mol L}^{-1}$   $\text{PO}_4$  after addition). Maximum nutrient concentrations measured in the fjord were  $1.73 \mu\text{mol L}^{-1}$   $\text{NO}_3$  and  $0.06 \mu\text{mol L}^{-1}$   $\text{PO}_4$ . Outgassing of  $\text{CO}_2$  and carbon fixation by phytoplankton caused a gradual  $p\text{CO}_2$  decline and pH increase in  $\text{CO}_2$ -enriched mesocosms (Fig. 3). The average pH before nutrient addition ranged between  $8.13 \pm 0.01$  in the control mesocosms and  $7.31 \pm 0.12$  in M9

**Table 1. Comparison of *E. huxleyi* cell counts and dimethylsulfide (DMS) and total dimethylsulfoniopropionate (DMSP<sub>T</sub>) concentration ranges and means for the mesocosm and the *E. huxleyi* culture experiments**All *E. huxleyi* counts show calcified cells only. The percentage changes in total measured DMS and DMSP<sub>T</sub> concentrations are also shown. NS, not significant

Experiment	<i>E. huxleyi</i> RCC1229 culture experiment		Mesocosm experiment		
$p\text{CO}_2$ treatment ( $\mu\text{atm}$ )	390	900	390	840	3000
<i>E. huxleyi</i> range (cells $\text{mL}^{-1}$ )	87 439–1 355 000	60 598–1 254 000	81–2004	58–1393	15–135
Nanophytoplankton (2–6 $\mu\text{m}$ ) range (cells $\text{mL}^{-1}$ )			2341–28 628	2373–29 412	2453–20 649
DMS range (nmol $\text{L}^{-1}$ )	6.5–345.8	11.5–366.6	0.4–4.9	0.1–2.4	0.1–0.8
DMS Mean ( $\pm$ s.d.) (nmol $\text{L}^{-1}$ )	74.5 $\pm$ 73.7	77.8 $\pm$ 83.4	1.5 $\pm$ 1.2	1.0 $\pm$ 0.6	0.4 $\pm$ 0.2
DMS percentage change		NS		–17	–60
DMSP <sub>T</sub> range (nmol $\text{L}^{-1}$ )	109.8–6233.6	144.1–6062.3	21.1–67.4	20.3–81.9	14.6–58.2
DMSP <sub>T</sub> mean ( $\pm$ s.d.) (nmol $\text{L}^{-1}$ )	1840.2 $\pm$ 1621.1	1769.0 $\pm$ 1546.5	46.0 $\pm$ 12.0	44.5 $\pm$ 15.6	28.8 $\pm$ 15.2
DMSP <sub>T</sub> percentage change		NS		–13	–32

**Fig. 3.** Daily measurements of  $\text{CO}_2$  partial pressure ( $p\text{CO}_2$ ) during the mesocosm experiment. Dashed lines indicate the three phases of the experiment: the initial bloom, the second bloom and the post-bloom phase. Blue lines indicate low  $p\text{CO}_2$  (280–390  $\mu\text{atm}$ ), grey lines mid-range  $p\text{CO}_2$  (560–1120  $\mu\text{atm}$ ) and red lines high  $p\text{CO}_2$  (1400–3000  $\mu\text{atm}$ ) treatments.

(3000  $\mu\text{atm}$ ), the highest  $p\text{CO}_2$  mesocosm. After nutrient addition, the pH ranged between  $8.14 \pm 0.01$  in the control mesocosms and  $7.49 \pm 0.05$  in the highest  $p\text{CO}_2$  mesocosm. The temperature varied between  $6.8^\circ\text{C}$  at the beginning and  $10.0^\circ\text{C}$  at the end of the experiment.

#### Changes in community composition

Three phases were identified from the fluorometric Chl-*a* data (Fig. 4a): phase 1 as the initial bloom before artificial nutrient addition, phase 2 as the artificial nutrient-induced bloom and phase 3 as post-bloom. The initial Chl-*a* concentrations in all mesocosms were  $2.2 \pm 0.1 \mu\text{g L}^{-1}$  at T1 and rapidly increased in a similar manner in all treatments during the phase 1 bloom (Fig. 4a), peaking on T3 in all mesocosms except for M9 (3000  $\mu\text{atm}$ ) which continued to increase until  $4.1 \mu\text{g L}^{-1}$  on T5. A clear differentiation between  $p\text{CO}_2$  treatments was seen after T3, with Chl-*a* concentrations higher in the high  $p\text{CO}_2$  treatment until the beginning of phase 2 at T9, after which they dropped below the Chl-*a* concentrations of the control and medium  $p\text{CO}_2$  mesocosms. During the phase 2 nutrient-induced bloom after T14, Chl-*a* concentrations were lower at high  $p\text{CO}_2$ , and peaked at  $\sim$ T19–T20, before declining through phase 3 until the end

of the experiment. Several different phytoplankton species were significant contributors to the total Chl-*a* throughout the experiment as measured by HPLC pigment data, including diatoms ( $\sim 35\%$ ), cryptophytes ( $\sim 22\%$ ), chlorophytes ( $\sim 20\%$ ) and haptophytes ( $\sim 19\%$ ; Fig. 4b). Other taxa, including cyanobacteria, dinoflagellates and chrysophytes made a minor ( $< 4\%$ ) contribution to the total Chl-*a*. Haptophyte equivalent Chl-*a* showed a peak in all  $p\text{CO}_2$  treatments during phase 1, with maximum concentrations of  $0.84 \mu\text{g L}^{-1}$  in the control mesocosms, and there were no significant differences between any treatments during this phase ( $F = 0.73$ ,  $P = 0.669$ ,  $n = 98$ ). The phase 1 haptophyte equivalent Chl-*a* was coincident with the peak in DMSP<sub>T</sub> concentrations (Fig. 5b). The difference between elevated  $p\text{CO}_2$  treatments became more apparent after the initial bloom (T7 to T17) and after the nutrient induced bloom in phase 2 (T22 to T29), with significantly lower haptophyte equivalent Chl-*a* concentrations in the higher  $p\text{CO}_2$  treatments ( $F = 16.74$ ,  $P < 0.01$ ,  $n = 189$ ) from T9 compared to the low and medium  $p\text{CO}_2$  mesocosms. During the period T3 to T10, mean net growth rates for the haptophytes in the three high  $p\text{CO}_2$  mesocosms (1400–3000  $\mu\text{atm}$ ) were  $-0.2 \text{ day}^{-1}$ , compared to the mean net growth rate in the low  $p\text{CO}_2$  mesocosms (280–390  $\mu\text{atm}$ ) of  $-0.06 \text{ day}^{-1}$ . Haptophyte growth rates during the artificial bloom in phase 2 were subsequently higher in the high  $p\text{CO}_2$  mesocosms over the period T10 to T20 at  $0.1 \text{ day}^{-1}$  compared to  $0.02 \text{ day}^{-1}$  in the low  $p\text{CO}_2$  mesocosms and  $0.06 \text{ day}^{-1}$  in the medium (540–1120  $\mu\text{atm}$ ) mesocosms, but overall haptophyte Chl-*a* remained lower throughout phase 2 into phase 3. The mean calculated percentage contribution of the haptophyte Chl-*a* to total Chl-*a* was  $25 \pm 11\%$  in the low  $p\text{CO}_2$  mesocosms, but  $15 \pm 5\%$  in the highest, and this difference was pronounced in the post-bloom periods (Fig. 4c).

Calcified (C-form) *E. huxleyi* was the only haptophyte to be identified and enumerated using flow cytometry (Fig. 4d) however this method was not able to identify individual non-calcified haptophyte species; all these were combined in the small nanophytoplankton (2–6  $\mu\text{m}$ ) group with *E. huxleyi* (Fig. 4e). The abundance of calcified *E. huxleyi* cells increased during phases 2 and 3 when the majority of other groups declined in abundance. *E. huxleyi* peaked on T29 in the control (280  $\mu\text{atm}$ ) at  $\sim 3000 \text{ cells mL}^{-1}$ , and a distinct effect of  $p\text{CO}_2$  treatment was observed, with significantly lower abundance in the high  $p\text{CO}_2$  mesocosms ( $F = 13.45$ ,  $P < 0.01$ ,  $n = 112$ ). The nanophytoplankton group (2–6  $\mu\text{m}$ ) showed a similar pattern to the haptophyte equivalent Chl-*a* with a peak during each bloom period, but did not show significantly lower nanophytoplankton

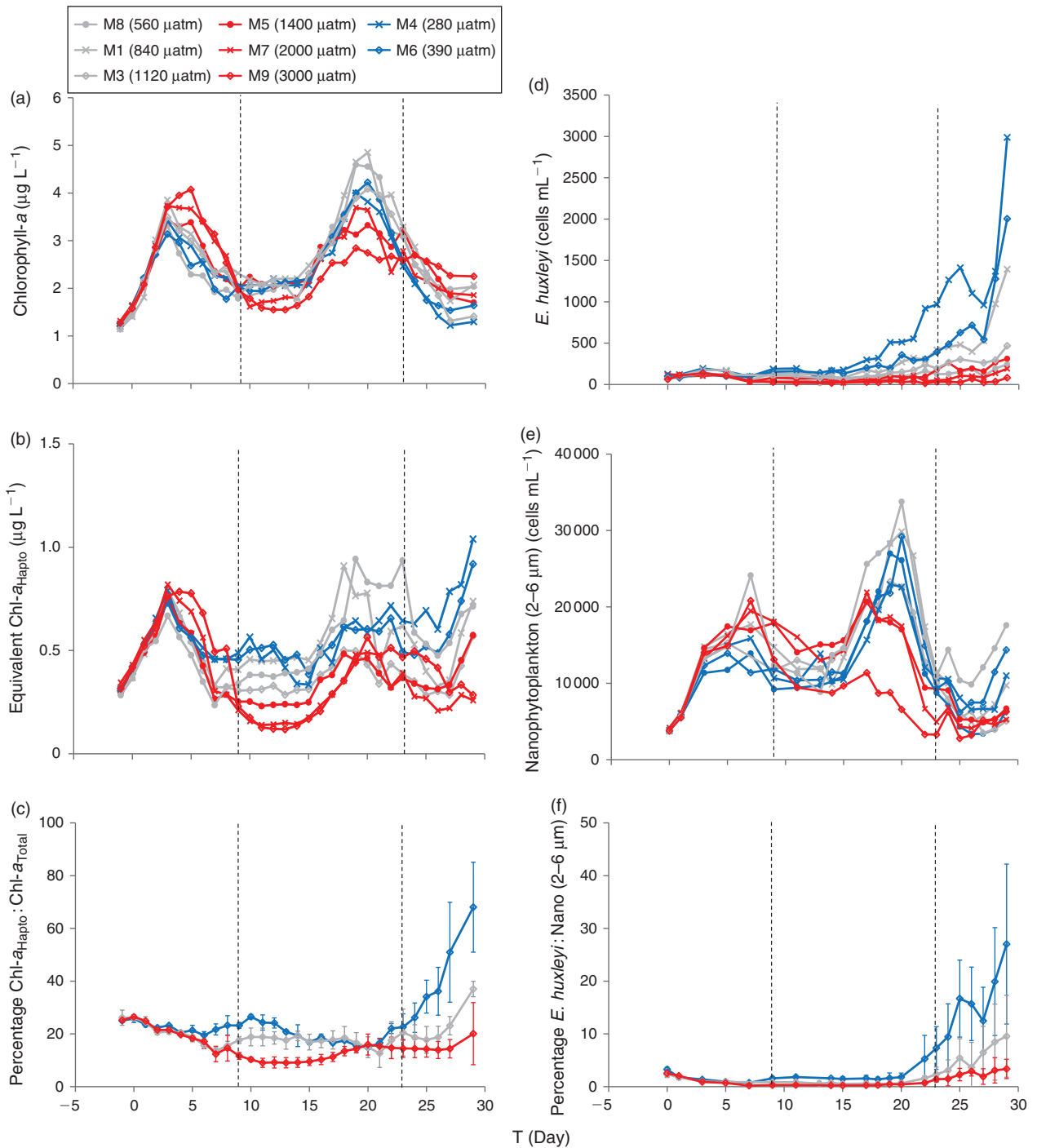


**Fig. 4.** Temporal changes in (a) chlorophyll-*a* (Chl-*a*) ( $\mu\text{g L}^{-1}$ ), (b) haptophyte equivalent Chl-*a* ( $\mu\text{g L}^{-1}$ ), (c) percentage haptophyte Chl-*a* to total Chl-*a*, (d) calcified *E. huxleyi* cell abundance (cells  $\text{mL}^{-1}$ ), (e) small nanophytoplankton including *E. huxleyi* (2–6  $\mu\text{m}$ ; cells  $\text{mL}^{-1}$ ) and (f) percentage *E. huxleyi*: small nanophytoplankton during the mesocosm experiment. Dashed lines indicate the three phases of the experiment: the initial bloom, the second bloom and the post-bloom phase. Blue lines indicate the low (280–390  $\mu\text{atm}$ ), grey lines the mid-range (560–1120  $\mu\text{atm}$ ) and red lines the high  $p\text{CO}_2$  partial pressure ( $p\text{CO}_2$ ) treatments (1400–3000  $\mu\text{atm}$ ). Error bars show the standard deviation between all mesocosms of low, medium and high  $p\text{CO}_2$ .

abundance at high  $p\text{CO}_2$  during the post-bloom period of phase 2 (T9–T15) directly following the initial bloom, which was notable in the haptophyte equivalent Chl-*a*. After T15, significantly lower cell abundance was identified in the highest  $p\text{CO}_2$  mesocosms, yet a higher abundance was seen in the medium  $p\text{CO}_2$  mesocosms compared to the control. Net nanophytoplankton growth rates were comparable between all mesocosms

for the period T5 to T15, in contrast to the haptophyte Chl-*a*, yet were lower in the high  $p\text{CO}_2$  mesocosms during the period T15 to T20. Nanophytoplankton abundance ranged from  $\sim 3000$  to  $33\,500$  cells  $\text{mL}^{-1}$  in all mesocosms, with maximum abundance in M8 (560  $\mu\text{atm}$ ) during phase 2. Calcified *E. huxleyi* cells contributed less than 5% to the total nanophytoplankton during phases 1 and 2 in all  $p\text{CO}_2$  treatments, but increased in the low

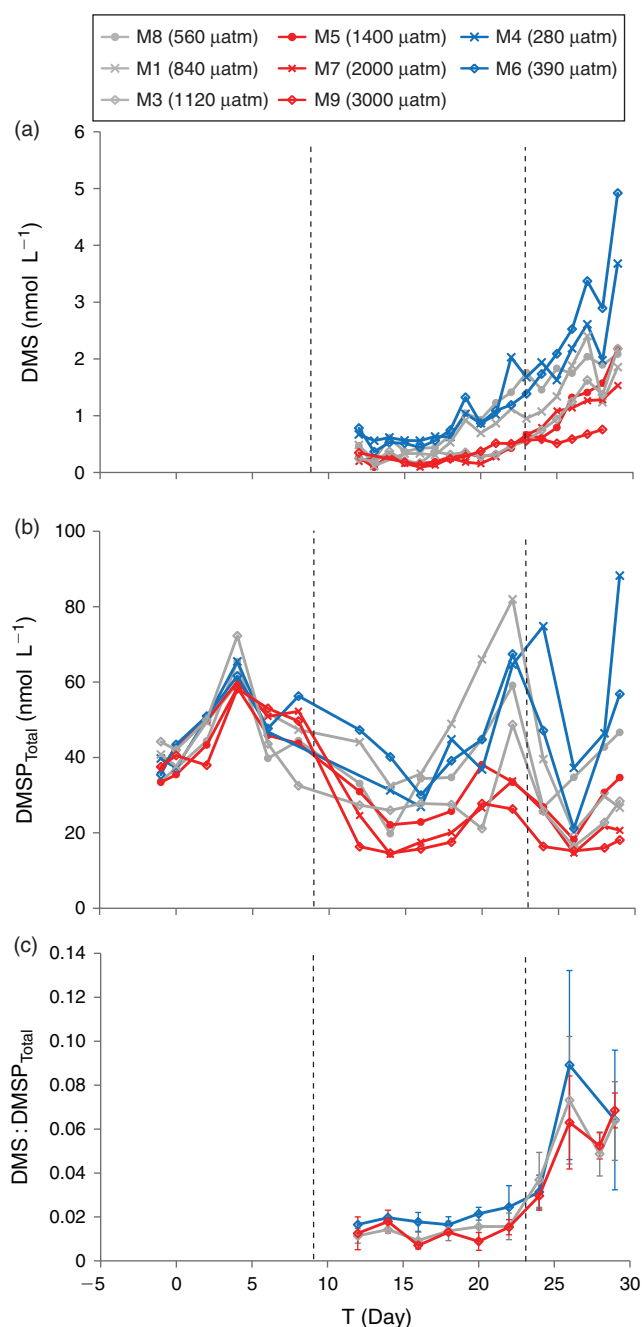


**Fig. 5.** Temporal changes in (a) dimethylsulfide (DMS) ( $\text{nmol L}^{-1}$ ) and (b) total dimethylsulfoniopropionate (DMSP<sub>T</sub>) ( $\text{nmol L}^{-1}$ ) with a single analysis per treatment. Blue lines indicate the low  $\text{CO}_2$  partial pressure ( $p\text{CO}_2$ ) treatments (280–390  $\mu\text{atm}$ ), grey lines the mid-range  $p\text{CO}_2$  treatments (560–1120  $\mu\text{atm}$ ) and red lines the high  $p\text{CO}_2$  treatments (1400–3000  $\mu\text{atm}$ ). The DMS-to-DMSP<sub>T</sub> ratio was calculated during phases 2 and 3 of the experiment (c) with error bars showing the standard deviation between all mesocosms of low, medium and high  $p\text{CO}_2$ . Dashed lines indicate the three phases of the experiment.

and medium  $p\text{CO}_2$  treatments to 27% at the end of phase 3 (Fig. 4f).

### DMS

DMS concentrations were measured from T12 to T29 for the mesocosms only in phases 2 and 3 (Fig. 5a). Until T19, DMS concentrations were below  $1 \text{ nmol L}^{-1}$  and from T20 onwards it increased in all  $p\text{CO}_2$  treatments. A clear effect of increased

$p\text{CO}_2$  is seen from the start of measurements on T12, with DMS concentrations in the highest  $p\text{CO}_2$  treatments (2000 and 3000  $\mu\text{atm}$ ) significantly lower than the low (280 and 390  $\mu\text{atm}$ ) and medium  $p\text{CO}_2$  (560, 840 and 1120  $\mu\text{atm}$ ) conditions ( $F = 5.52$ ,  $P < 0.01$ ,  $n = 175$ ), and these trends continued until T29. Maximum DMS concentrations were reached in M6 (390  $\mu\text{atm}$ ) on T29 at  $4.9 \text{ nmol L}^{-1}$ , compared to  $0.76 \text{ nmol L}^{-1}$  measured in M9 (3000  $\mu\text{atm}$ ) on T28. During phases 2 and 3, DMS concentrations in the high  $p\text{CO}_2$  treatments were 60% lower than the control and the medium  $p\text{CO}_2$  treatments 33% lower. Mean DMS concentrations plotted against the mean  $p\text{CO}_2$  for phases 2 and 3 showed a clear decreasing relationship as  $p\text{CO}_2$  increased (Fig. 6a;  $\rho = -0.595$ ,  $P < 0.01$ ,  $n = 140$ ), however with only three mesocosms at  $p\text{CO}_2$  higher than 1000  $\mu\text{atm}$ , it is difficult to determine the exact nature of the DMS– $p\text{CO}_2$  relationship at these high  $p\text{CO}_2$ .

### Total DMSP

DMSP<sub>T</sub> was measured on alternate days from T1 and showed different patterns to DMS (Fig. 5b). DMSP<sub>T</sub> concentrations were similar in all treatments on T1 ( $38.5 \pm 4.3 \text{ nmol L}^{-1}$  mean), and increased to a peak on T4, after which concentrations decreased. No difference between mesocosms was identified during phase 1 for DMSP<sub>T</sub> ( $F = 0.42$ ,  $P = 0.916$ ,  $n = 58$ ). A difference between mesocosms was more apparent for DMSP<sub>T</sub> during phases 2 and 3, with concentrations in the high (1400–3000  $\mu\text{atm}$ ) and medium  $p\text{CO}_2$  treatments (560–1120  $\mu\text{atm}$ ) 32 and 14% lower respectively than the low  $p\text{CO}_2$  mesocosms during both phases. This change seems to have been driven by the net DMSP production rate over the period T5 to T12, where the high  $p\text{CO}_2$  mesocosms (1400–3000  $\mu\text{atm}$ ) showed a loss rate of  $-0.12 \text{ day}^{-1}$  compared to the low  $p\text{CO}_2$  mesocosms (280–390  $\mu\text{atm}$ ) at  $-0.04 \text{ day}^{-1}$ . This higher loss rate, similar to that of the haptophyte equivalent Chl-*a*, influences the concentrations in the later part of phase 2 and during phase 3: DMSP<sub>T</sub> concentrations increased to a peak at T22 in all treatments, with the highest concentrations of  $81.8 \text{ nmol L}^{-1}$  in M1 (840  $\mu\text{atm}$ ) but the lowest at  $26.3 \text{ nmol L}^{-1}$  in M9 (3000  $\mu\text{atm}$ ). DMSP<sub>T</sub> concentrations then decreased at the start of phase 3, before increasing again in all treatments on T29, with the lowest concentrations measured in the highest  $p\text{CO}_2$  treatments. A summary of the DMS, DMSP and relevant cell abundance is given in Table 1.

### Relationships between DMS, DMSP and biological parameters

The community composition proxies (HPLC pigments and flow cytometry data) were analysed alongside the DMS and DMSP data to determine the potential sources of DMS and DMSP within the mesocosm communities. Using Spearman's rank correlation analysis, concentrations of DMS and DMSP<sub>T</sub> showed significant positive correlation to each other ( $\rho = 0.339$ ,  $P < 0.01$ ,  $n = 135$ ), and the ratio between the two compounds (Fig. 5c) was reasonably stable below 0.02 in all treatments during phase 2, but increased to  $\sim 0.06$  in phase 3 corresponding to an increase in DMS concentration. The ratio of DMS to DMSP<sub>T</sub> was unaffected by  $\text{CO}_2$  treatment: mean ratios were plotted against mean  $p\text{CO}_2$  in all mesocosms, and showed no change with increasing  $p\text{CO}_2$  (Fig. 6c;  $\rho = 0.289$ ,  $P = 0.083$ ,  $n = 62$ ).

DMSP<sub>T</sub> showed positive correlation with Chl-*a* ( $\rho = 0.400$ ,  $P < 0.01$ ,  $n = 117$ ), and an examination of the mean DMSP<sub>T</sub>-to-Chl-*a*<sub>Hapto</sub> ratio for each mesocosm plotted against mean



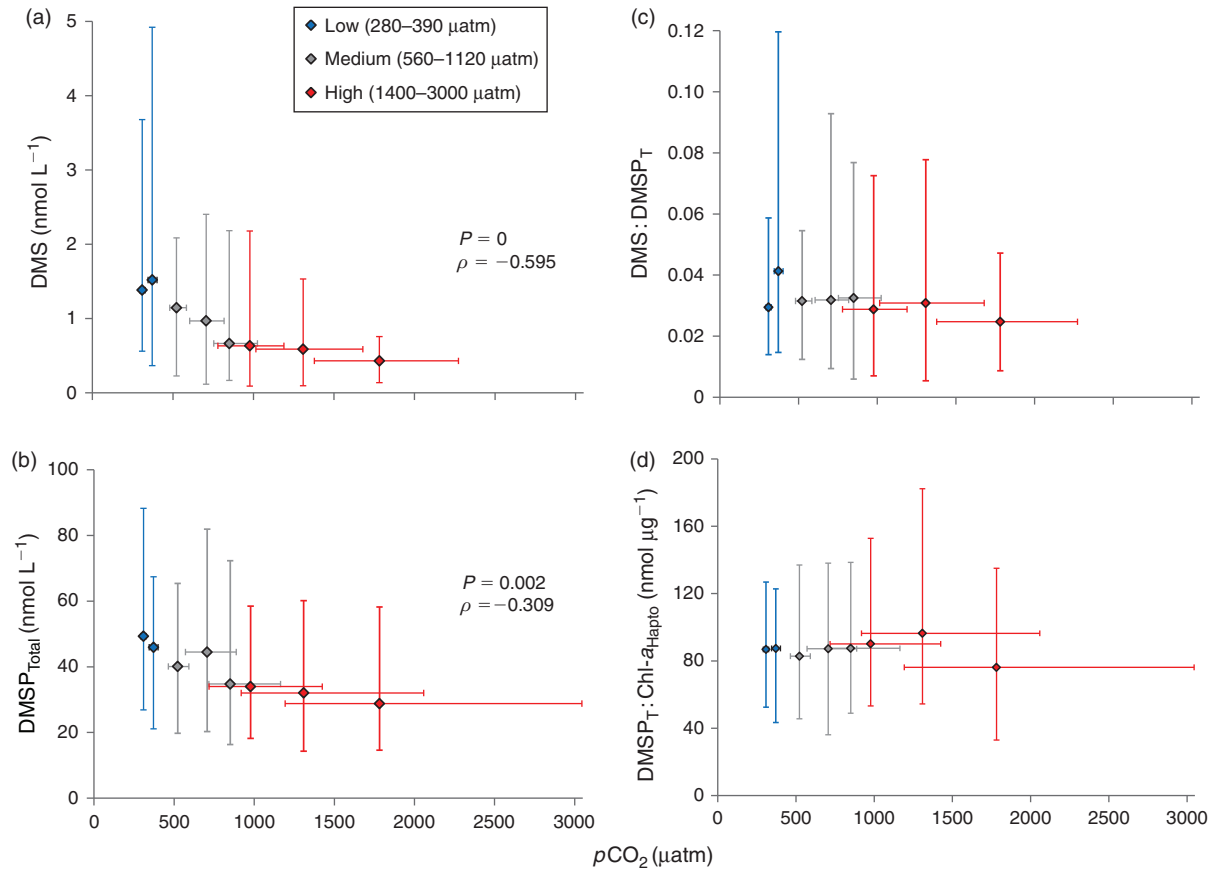


**Fig. 6.** Relationships between  $\text{CO}_2$  partial pressure ( $p\text{CO}_2$ ) and (a) mean dimethylsulfide (DMS) concentration ( $\text{nmol L}^{-1}$ ), (b) mean total dimethylsulfoniopropionate ( $\text{DMSP}_T$ ) concentration ( $\text{nmol L}^{-1}$ ), (c) mean DMS-to- $\text{DMSP}_T$  ratio and (d) mean  $\text{DMSP}_T$ -to-chlorophyll-*a* (Chl-*a*) ratio ( $\text{nmol } \mu\text{g}^{-1}$ ) for the low (blue; 280–390  $\mu\text{atm}$ ), medium (grey; 540–1120  $\mu\text{atm}$ ) and high (red; 1400–3000  $\mu\text{atm}$ )  $p\text{CO}_2$  treatments, plotted against the mean  $p\text{CO}_2$  in each mesocosm. Error bars show the range of the data on the horizontal and vertical axes. Where significant, the Spearman's rank correlation coefficients ( $\rho$ ) for the relationships between the variables are shown, with the corresponding  $p$ -value.

$p\text{CO}_2$  for the entire experiment showed no effect of increased  $p\text{CO}_2$  (Fig. 6d;  $\rho = -0.01$ ,  $P = 0.920$ ,  $n = 99$ ). DMS showed negative correlation with total Chl-*a* ( $\rho = -0.406$ ,  $P < 0.01$ ,  $n = 136$ ). Correlations between DMS and all phytoplankton abundances and Chl-*a* contributors showed that DMS concentrations correlated only with the haptophyte-equivalent Chl-*a* ( $\rho = 0.508$ ,  $P < 0.01$ ,  $n = 126$ ) and calcified *E. huxleyi* abundance ( $\rho = 0.615$ ,  $P < 0.01$ ,  $n = 136$ ), however the latter only reached 3000 cells  $\text{mL}^{-1}$  in M4 (290  $\mu\text{atm}$ ) on T29 (Fig. 4d).  $\text{DMSP}_T$  correlation with haptophyte equivalent Chl-*a* was also strong ( $\rho = 0.635$ ,  $P < 0.01$ ,  $n = 121$ ), with relatively weak correlation with the nanophytoplankton ( $\rho = 0.283$ ,  $P < 0.01$ ,  $n = 117$ ) and no relationship with calcified *E. huxleyi* abundance. In addition, there was weak correlation between  $\text{DMSP}_T$  and the diatoms ( $\rho = 0.301$ ,  $P < 0.01$ ,  $n = 121$ ). The ratios of DMS and  $\text{DMSP}_T$  to nanophytoplankton (2–6  $\mu\text{m}$ ) abundance (Figs 7a, b) and haptophyte equivalent Chl-*a* (Fig. 7c, d) were calculated on a daily basis, and showed a limited effect of elevated  $p\text{CO}_2$ . The haptophytes were significant contributors to the DMSP pool given the strong correlations with  $\text{DMSP}_T$  and high contribution to the total Chl-*a* (Fig. 4c), whereas calcified *E. huxleyi* contributed to only a small percentage of the total haptophyte assemblage (Fig. 4f) and subsequently the DMSP production. Calcified *E. huxleyi* were of greater importance to DMSP production during phase 3 of the experiment when the abundance was highest. It is highly likely that a large proportion

of the nanophytoplankton (2–6  $\mu\text{m}$ ; Fig. 4e) were non-calcified DMSP-producing haptophyte cells, although no determination of species composition could be made. Non-calcified *E. huxleyi* cannot be distinguished from other non-calcified haptophytes of the same size by flow cytometry (A. Larsen, pers. comm.).

## Discussion

Several mesocosm experiments investigating the effect of elevated  $p\text{CO}_2$  on the community structure have been performed, and several of these have measured the effects on DMS and DMSP concentrations. These are summarised in Table 2, alongside experiments on clonal *E. huxleyi* cultures which also measured DMS and DMSP v.  $\text{CO}_2$  concentrations. The ranges in DMS and DMSP concentrations from the mesocosm experiment in this study are within those seen in previous Bergen mesocosm studies,<sup>[24,25,28,53,54]</sup> and the Korean and Svalbard mesocosm experiments, where microbial communities from neither location contained a significant abundance of *E. huxleyi*.<sup>[23,26,27]</sup> During this experiment no single group dominated the community at any time; there were high abundances of diatoms, cryptophytes, chlorophytes and haptophytes, but only the haptophytes were significantly correlated with DMSP concentrations. The  $p\text{CO}_2$  range used by us was broader than in any previous investigation, with mesocosms at 2000 and 3000  $\mu\text{atm}$ ; the aim being to identify trends of different

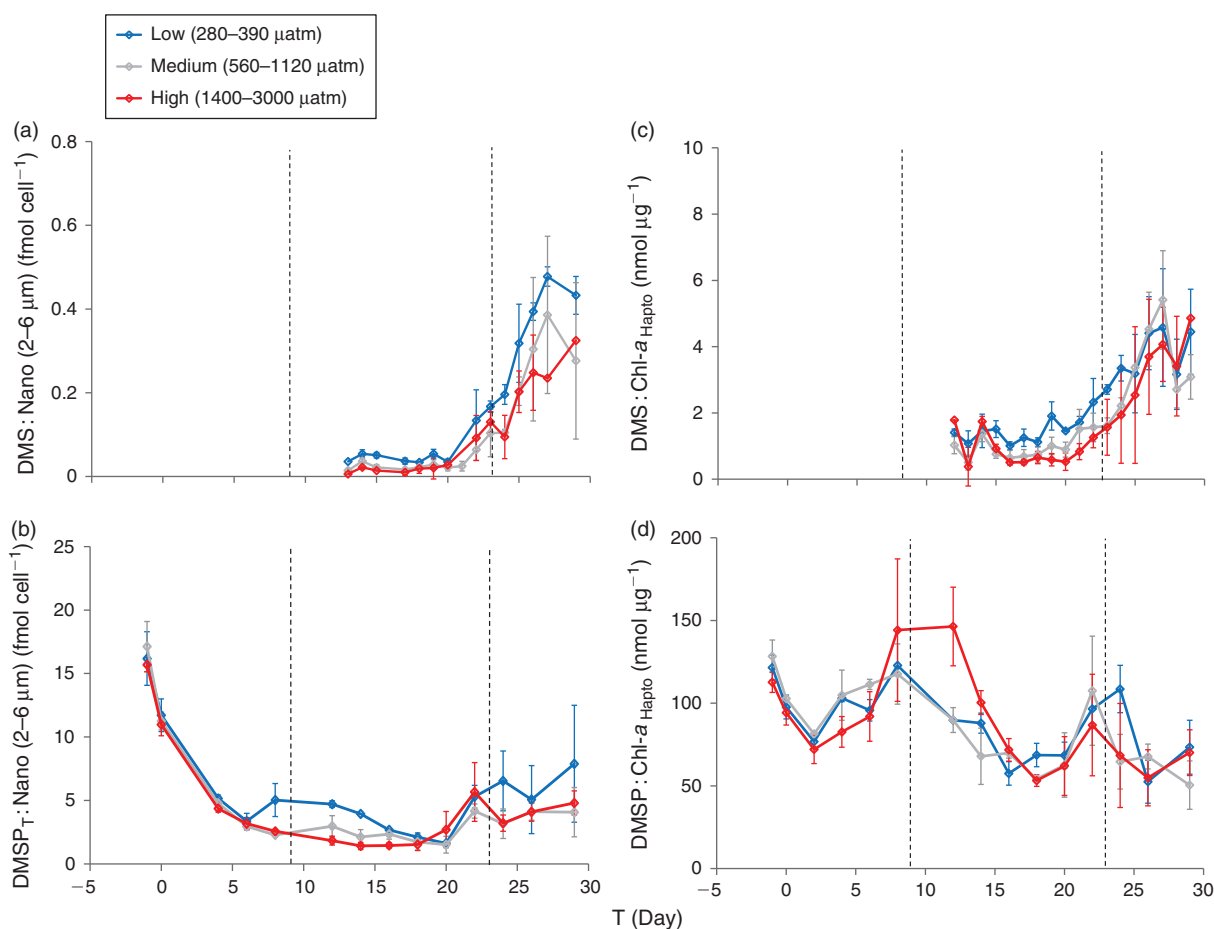


**Fig. 7.** Mean ratios of (a) dimethylsulfide (DMS) to nanophytoplankton (2–6  $\mu\text{m}$ ) ( $\text{fmol cell}^{-1}$ ), (b) total dimethylsulfoniopropionate (DMSP<sub>T</sub>) to nanophytoplankton (2–6  $\mu\text{m}$ ) including *E. huxleyi* ( $\text{fmol cell}^{-1}$ ), (c) DMS to haptophyte equivalent chlorophyll-*a* (Chl-*a*) ( $\text{nmol } \mu\text{g}^{-1}$ ) and (d) DMSP<sub>T</sub> to haptophyte equivalent Chl-*a* ( $\text{nmol } \mu\text{g}^{-1}$ ) for three different  $p\text{CO}_2$  conditions: low (blue; 280  $\mu\text{atm}$ ), medium (grey; 390–1120  $\mu\text{atm}$ ) and high (red; 1400–3000  $\mu\text{atm}$ ). Error bars show the standard deviation between all mesocosms of low, medium and high  $p\text{CO}_2$ .

community parameters beyond the  $p\text{CO}_2$  projected for the year 2100. The change in  $p\text{CO}_2$  in the system occurred over 3–5 days (Fig. 3), and the community response would have favoured those species with less efficient carbon concentrating mechanisms (CCMs),<sup>[55–57]</sup> as well as those better suited to rapid environmental change. Over the course of the experiment, the  $p\text{CO}_2$  decreased in all the treated mesocosms, with the result that the artificial bloom was at a lower mean  $p\text{CO}_2$  for each mesocosm than the initial bloom, but the communities would have been exposed to the perturbed conditions for a longer time period. Differences were identified between treatments for several community parameters: chlorophytes, picoeukaryotes and cyanobacteria showed a strong positive response in high  $p\text{CO}_2$ , whereas haptophyte and diatom growth was negatively affected at the highest  $p\text{CO}_2$ . These responses were more pronounced during the latter phases of the experiment.

#### Community development and *E. huxleyi* growth

The total Chl-*a* concentrations in the mesocosms showed both positive and negative effects to  $\text{CO}_2$  during the three different phases, a scenario which was also identified during a mesocosm experiment in Svalbard,<sup>[52]</sup> and is a result of different phytoplankton assemblages responding to elevated  $p\text{CO}_2$  at different times of the experiment. Of importance to this investigation,

haptophyte-equivalent Chl-*a*, nanophytoplankton and calcified *E. huxleyi* cells showed reduced abundance under increased  $p\text{CO}_2$  during phases 2 and 3, either as a direct result of  $\text{CO}_2$  on the groups, or as a result of differential nutrient-induced competition between groups such as diatoms and picoeukaryotes at the higher availability of DIC,<sup>[52,58,59]</sup> as was previously identified during the Svalbard mesocosm experiment in 2010. In contrast, Endres et al.<sup>[31]</sup> identified significantly higher marine bacterial abundance and activity in the high  $p\text{CO}_2$  mesocosms during the same period. Calcified *E. huxleyi* cell counts during the mesocosm experiment were unexpectedly low (up to 3000 cells  $\text{mL}^{-1}$ ) in comparison to some previous experiments (e.g. up to 70 000 cells  $\text{mL}^{-1}$  in Steinke et al.<sup>[53]</sup> and up to 50 000 cells  $\text{mL}^{-1}$  in Delille et al.<sup>[60]</sup>) and there was no analysis performed on calcification rates in *E. huxleyi* or evaluating coccolith formation. Analysis of the phytoplankton community by flow cytometry was unable to identify other calcified coccolithophore species than *E. huxleyi*, however the mismatch between the pattern of haptophyte equivalent Chl-*a* and the abundance of calcified *E. huxleyi* cells identified by flow cytometry indicate the presence of non-calcified haptophyte cells which were enumerated only as nanophytoplankton (2–6  $\mu\text{m}$ ). Previous investigations at Espesgrend Marine Biological Station have identified non-calcified *E. huxleyi* cells within the coastal phytoplankton community.<sup>[61]</sup> Indeed, in a

**Table 2. Comparison of dimethylsulfide (DMS) and dimethylsulfoniopropionate (DMSP) concentrations from this study and previous CO<sub>2</sub> partial pressure (pCO<sub>2</sub>) perturbation experiments**  
 ND, not detected; NC, no change. Asterisks indicate concentrations were given in millimoles of DMSP per litre

Experiment	Location or culture strain	pCO <sub>2</sub> range (µatm)	Range DMS (nmol L <sup>-1</sup> )	Percentage change DMS	Range DMSP (nmol L <sup>-1</sup> )	Percentage change DMSP	Reference
Bergen Mesocosm Experiment, 2011	Raunesfjorden, Norway	280–3000	0.09–4.92	-60	14.3–88.2	-32	This study
Korean Mesocosm Experiment 2, 2012	Jangmok, Korea	160–830	1.0–100	-82	10–350	-71	Park et al. <sup>[27]</sup>
EPOCA Svalbard, 2010	Kongsfjorden, Svalbard	180–1420	ND–14	-60	ND–80	50	Archer et al. <sup>[23]</sup>
Korean Mesocosm Experiment 1, 2008	Jangmok, Korea	400–900	1–12	80	No data	No data	Kim et al. <sup>[26]</sup>
NERC Microbial Metagenomics Experiment, 2006	Raunesfjorden, Norway	300–750	ND–50	-57	30–500	-24	Hopkins et al. <sup>[24]</sup>
PeECE III, 2005	Raunesfjorden, Norway	300–750	ND–35	NC	10–500	NC	Vogt et al. <sup>[28]</sup>
PeECE II, 2003	Raunesfjorden, Norway	300–750	5–30	-40	ND–300	-40	Avogustidi et al. <sup>[25]</sup>
UKOA European Shelf Cruise, 2011	NW European Shelf	340–1000	0.5–12	225	5–80	-52	Hopkins and Archer <sup>[71]</sup>
<i>E. huxleyi</i> Batch Experiments	CCMP1516	370–760	0.1–2.5	-90	500–4000	-60	Avogustidi et al. <sup>[25]</sup>
<i>E. huxleyi</i> pH stat experiment	CCMP 373	385–1000	2.5–5.0	NC	84.0–200	NC	Arnold et al. <sup>[69]</sup>
<i>E. huxleyi</i> Semi-continuous Experiment	RCC1242	390–790			100–270*	30	Spielmeier and Pohmert <sup>[65]</sup>
<i>E. huxleyi</i> Semi-continuous Experiment	RCC1731	390–790			50–60*	NC	

mesocosm experiment in the Raunefjord in 2008, a significant number (up to 40 000 cells mL<sup>-1</sup>) of non-calcified haptophyte cells were identified in the natural population through the use of COD-FISH (combined CaCO<sub>3</sub> optical detection with fluorescent in-situ hybridisation) techniques.<sup>[62,63]</sup>

Calcification rates were not measured during our mesocosm and laboratory culture experiments, but previous mesocosm studies have identified reductions in calcification under elevated pCO<sub>2</sub>,<sup>[60,64]</sup> which has been suggested as a negative feedback on surface water pCO<sub>2</sub>.<sup>[10]</sup> As mentioned above, non-calcified *E. huxleyi* cells do occur in natural and mesocosm assemblages, but their presence is not indicative of lower calcification rates. Overall, understanding of the non-calcified life-stages of *E. huxleyi* is very scant, and requires further investigation into the physiological changes that occur in the different forms (haploid and diploid, calcified and non-calcified). In addition, other non-calcifying haptophytes were likely present in the community and contributing to the haptophyte Chl-*a* signal. In terms of DMSP production, a single investigation found that DMSP production was increased by up to 0.4 pg cell<sup>-1</sup> in a non-calcified *E. huxleyi* strain (N-Form diploid RCC1242) under 790 µatm pCO<sub>2</sub> compared to an ambient pCO<sub>2</sub> control, whereas a calcified strain (C-form diploid RCC1731) showed no CO<sub>2</sub> effect.<sup>[65]</sup> Further studies of DMSP production from diploid calcified and non-calcified (haploid and diploid) strains in the laboratory and non-calcified cells in the field are certainly warranted, as well as further investigation into the DMSP production of the haploid life-stages, which has never been previously investigated.

There have been several studies on the effect of elevated pCO<sub>2</sub> on different strains of *E. huxleyi*, isolated from different geographical areas,<sup>[9,65–70]</sup> but never using the strain RCC1229. This strain was chosen because of its origins in the North Sea close to the Bergen coast (58.42°N, 3.21°E), and likely similar genotype to the natural *E. huxleyi* identified during the Bergen mesocosm experiment. Despite this, calcified cell abundance in the mesocosms showed a significant decrease at 840 µatm pCO<sub>2</sub>, but no such effect was identified during the culture experiments at a comparable pCO<sub>2</sub>. While the culture experiments were nutrient replete, *E. huxleyi* within the mesocosms showed significant growth during phase 3 after the artificial bloom, when concentrations of inorganic nitrate and phosphate were low. Although RCC1229 was isolated close to the location of the mesocosm experiment, there is still likely significant genetic difference between the strain and the wild population. The physiological responses between different strains to increased pCO<sub>2</sub> have not been uniform: in general carbon fixation has increased,<sup>[65,68,70,71]</sup> but three strains investigated by Langer et al.<sup>[66]</sup> showed the opposite effect. *E. huxleyi* has shown varying sensitivity of growth rate to pCO<sub>2</sub> in the laboratory and the field. A previous mesocosm experiment identified decreased net specific growth rate from 0.5 to 0.43 day<sup>-1</sup> in the highest pCO<sub>2</sub> mesocosms,<sup>[72]</sup> and the reduced haptophyte equivalent Chl-*a* concentrations and calcified *E. huxleyi* abundance values seen in our medium and high pCO<sub>2</sub> mesocosms support this. However, in the laboratory, varying responses have been identified for different *E. huxleyi* strains where growth rates either increased,<sup>[9,70,73]</sup> remained unchanged as in this study<sup>[65,69,74]</sup> or decreased.<sup>[66,75,76]</sup> Specific growth rates during the *E. huxleyi* RCC1229 experiment were lower (0.48 day<sup>-1</sup> for the 900 µatm pCO<sub>2</sub> treatment and 0.47 day<sup>-1</sup> for the ambient CO<sub>2</sub> control) than found previously for that strain under near-identical growth conditions at the same

temperature ( $0.67 \text{ day}^{-1}$ ),<sup>[77]</sup> and was likely a result of methodological differences in culturing which can be a significant problem in comparing growth rates between different investigations.<sup>[78]</sup> The growth rate of calcified RCC1229 was not affected by  $900 \mu\text{atm } p\text{CO}_2$ , whereas the abundance of calcified cells decreased in the  $840 \mu\text{atm } p\text{CO}_2$  mesocosm. A significant shift to a larger cell size was identified during the RCC1229 culture experiment, which reinforces the findings of Arnold et al.<sup>[69]</sup> using non-calcifying strain CCMP373, suggesting that the cell size increase is not linked to additional coccolith production. Increased particulate organic carbon (POC) production at higher  $p\text{CO}_2$  has been linked to larger cell size.<sup>[79]</sup> The long-term studies of Lohbeck et al.<sup>[80]</sup> with over 500 generations of single and multi-clonal experiments found a decrease in cell size as  $p\text{CO}_2$  increased. These variations in growth rate and carbon fixation limit the use of a single *E. huxleyi* strain as a representative of all coccolithophores and haptophytes in the natural environment. In contrast, Franklin et al.<sup>[81]</sup> identified *E. huxleyi* as a good model for the coccolithophores as a whole, particularly in terms of DMSP production, but only examined two strains of *E. huxleyi*. Comparison of the experiments described here and existing studies on *E. huxleyi* suggest sufficient genetic diversity and plasticity in natural populations to at least partially adapt as surface water  $p\text{CO}_2$  increases.<sup>[80]</sup> *E. huxleyi* has shown significant advancement into polar waters since the first half of the 20th century because of expansion of the thermal window,<sup>[82,83]</sup> but the effect of ocean acidification on these blooms is still unclear. Future laboratory high  $p\text{CO}_2$  experiments should focus on species other than *E. huxleyi*, and on other significant DMSP producers which would allow for better analysis of community development in mesocosm studies such as this.

#### DMS and DMSP

DMSP concentrations measured in the mesocosms were strongly correlated with haptophyte equivalent Chl-*a* and nanophytoplankton abundance, but not calcified *E. huxleyi* abundance. Although these groups were unlikely to be the sole producers of DMSP, the negative effect of acidification on the bloom dynamics of these groups had significant influence on the lower DMSP concentrations measured in the high  $p\text{CO}_2$  mesocosms. DMSP correlated well with haptophyte Chl-*a*, with DMSP-to-Chl-*a*<sub>Hapto</sub> ratios of 10–60  $\text{nmol } \mu\text{g}^{-1}$  in strong agreement with those identified in a previous mesocosm experiment.<sup>[28]</sup> During the period T9–T14, the increased DMSP-to-Chl-*a*<sub>Hapto</sub> ratio in the high  $p\text{CO}_2$  mesocosms was a result of the lower haptophyte Chl-*a*, likely attributable to nutrient competition, particularly with picoeukaryotes at the higher  $p\text{CO}_2$  mesocosms during the natural post-bloom phase, and not a direct result of elevated  $p\text{CO}_2$ . The DMS-to-DMSP ratio was unaffected by the change in  $p\text{CO}_2$  (Fig. 6c), and therefore the reduction in DMSP would explain a proportion of the 60% reduction in DMS concentrations measured in the mesocosms. In several previous mesocosm experiments, measured DMS and DMSP concentrations were found to be negatively affected by increased  $p\text{CO}_2$ ,<sup>[24,25,27]</sup> but in others the effect was either temporally offset,<sup>[28]</sup> or showed differential responses in DMS and DMSP.<sup>[23]</sup> Although the DMSP<sub>T</sub> concentrations in the RCC1229 *E. huxleyi* experiment showed no significant difference between treatments, DMSP<sub>T</sub> was 12% lower in the  $900 \mu\text{atm } p\text{CO}_2$  treatment when normalised to CV (Fig. 2d). In contrast, pH-stat laboratory experiments on clonal *E. huxleyi* cultures showed either no effect of elevated

$p\text{CO}_2$ , or increased DMSP production<sup>[65,69,84]</sup> when the  $p\text{CO}_2$  was equivalent to that of our mid or high range mesocosm experiments ( $>800 \mu\text{atm}$ ). DMS concentrations in the laboratory cultures showed no significant difference when normalised to CV, with no pronounced differences in *E. huxleyi* biomass, implying that microbial interaction occurs within the mesocosms which is limited in the cultures. Clearly, mesocosm experiments assess the community response to increasing  $p\text{CO}_2$  whereas laboratory experiments investigate the physiological changes within a single species and the effect these have on the production of DMSP and DMS; the greater response to acidification in the mesocosms compared to the laboratory experiment implies that there is a strong community interaction in the net production of DMS and DMSP. The DMSP producers showed no immediate DMSP response upon addition of the  $\text{CO}_2$ -enriched waters to the mesocosms (Fig. 7b,d) over T1 to T3, implying that DMSP production is not a direct response to changing environmental conditions.

The poor relationship of DMS with Chl-*a* has been reported several times, both regionally<sup>[85–87]</sup> and in data analysis–global modelling studies,<sup>[88]</sup> because of the likely differential DMSP synthesis of phytoplankton groups, variability in community DMSP-into-DMS conversion yields and DMS loss rate constants.<sup>[89]</sup> Total DMSP measured in the mesocosms included the intracellular particulate DMSP (DMSP<sub>P</sub>) and extracellular dissolved DMSP (DMSP<sub>D</sub>). DMS and DMSP<sub>T</sub> have often been found decoupled, particularly during the ‘summer paradox’ of delayed DMS maxima compared to DMSP maxima and phytoplankton maximum abundance,<sup>[22,90,91]</sup> driven by grazing-induced particulate DMSP transformation. DMSP is degraded through two separate pathways<sup>[92]</sup>: demethylation to methylmercaptpropionate (MMPA)<sup>[93]</sup> or cleavage to DMS with production of either acrylate or 3-hydroxypropionate through the ‘DMSP-lyase’ pathway,<sup>[92,94]</sup> and can be intracellular or extracellular by marine bacteria in the surrounding waters.<sup>[95,96]</sup> These routes regulate the gross DMS production rates in seawater, and thereby affect the flux of sulfur to the atmosphere. Previous studies on DMSP-lyase activity showed variations in the optimum pH, from pH 5 in several haptophyte *Phaeocystis* spp.<sup>[97]</sup> and coccolithophore *Gephyrocapsa oceanica*,<sup>[81]</sup> to pH 8 in the bacterium *Ruegeria lacuscaerulensis*<sup>[98]</sup> and *Pseudomonas doudoroffii*<sup>[99]</sup> and up to pH 10.5 in a further *Phaeocystis* strain.<sup>[100]</sup> The implication is that community production of DMS from the cleavage of DMSP is unlikely to be immediately affected by lowered pH as a result of ocean acidification, but individual species with optimal pH above 8 will find it increasingly difficult to cleave DMSP at higher atmospheric  $p\text{CO}_2$ .

The DMSP<sub>D</sub> pool supports 1–13% of bacterial carbon<sup>[18,101]</sup> and 3–100% of bacterial sulfur<sup>[18]</sup> demand, by the breakdown pathways diverting sulfur away from DMS production.<sup>[102,103]</sup> Increased consumption of the DMSP<sub>D</sub> pool by bacteria would affect not only the DMSP<sub>T</sub> concentrations but also reduce DMS production from the cleavage pathways. Bacterial transformation of DMS to dimethyl sulfoxide (DMSO) has been identified as the removal pathway for the majority of DMS,<sup>[104]</sup> further reducing the DMS concentrations during the greater bacterial activity at higher  $p\text{CO}_2$ .

In the laboratory experiments, bacterial abundance was kept low by treatment with antibiotics before the initial inoculation, and were checked by 4',6-diamidino-2-phenylindole (DAPI) staining at the end of the experiment, when bacterial abundances were found to be low. During the mesocosm experiment,

bacterial abundance increased by 28% in the high  $p\text{CO}_2$  treatments in comparison to the low  $p\text{CO}_2$  mesocosms, and showed three times higher leucine aminopeptidase activity as a proxy for bacterial enzyme hydrolysis.<sup>[31]</sup> This higher bacterial abundance at high  $p\text{CO}_2$  could result in greater consumption of DMSP from the dissolved phase as a greater bacterial abundance and activity is likely to drive an increased demand for sulfur sources, as well as drive greater conversion of DMS into DMSO. Bacterial loss processes for both DMS and DMSP could account for the lower concentrations of both compounds at elevated  $p\text{CO}_2$ , while not affecting the DMS-to-DMSP ratio.

During phase 3 of the experiment, there was an increase in DMS concentration which was not explained by corresponding increases in  $\text{DMSP}_T$  (Fig. 5c), haptophyte Chl-*a* (Fig. 7c) or nanophytoplankton abundance (Fig. 7a), but which was unaffected by elevated  $p\text{CO}_2$  (Fig. 6c) and implied that DMS turnover and loss processes were similar in all mesocosms. A study by Pinhassi et al.<sup>[105]</sup> in microcosms identified that DMSP was utilised as a sulfur source and removed by bacterioplankton more during the bloom phase (i.e. phase 2) than during senescence (i.e. phase 3), potentially resulting in greater availability of  $\text{DMSP}_D$  during phase 3 for conversion into DMS. Scarratt et al.<sup>[106]</sup> identified a direct relationship of DMS concentrations with  $\text{DMSP}_D$  in short-term incubations, which would imply a greater contribution of dissolved DMSP to the measured  $\text{DMSP}_T$  in phase 3 of the mesocosm experiment, after the artificial nutrient-induced bloom in phase 2.

## Summary

A significant reduction in DMS and DMSP concentrations was identified during a mesocosm experiment designed to study the effects of elevated  $p\text{CO}_2$  on a coastal phytoplankton community. The major DMSP producers were identified as nanophytoplanktonic haptophytes which showed lower biomass under elevated  $p\text{CO}_2$ . The same effect was not observed during laboratory culture experiments on a calcifying strain of *E. huxleyi* (RCC1229), which indicates that consumption and turnover of  $\text{DMSP}_D$  and DMS in surface waters at elevated  $p\text{CO}_2$  by the microbial community is as important as gross DMSP production in determining the concentrations of DMS and DMSP in (future) acidified waters. Elevated  $p\text{CO}_2$  affected the growth of calcified *E. huxleyi* and nanophytoplankton (2–6  $\mu\text{m}$ ) which would have contained non-calcified haptophyte cells, and the reduction in abundance significantly contributed to the lower DMSP concentrations at high  $p\text{CO}_2$ .

Several mesocosm studies, including this one, have shown that the phytoplankton community response to an increase in  $p\text{CO}_2$  has resulted in lower DMS concentrations than seen in the ambient  $p\text{CO}_2$  concentrations of today.<sup>[1]</sup> This response is representative of the exposure of the current phytoplankton community assemblage to a comparatively rapid increase in  $p\text{CO}_2$ , and does not reflect the adaptation likely to occur in phytoplankton communities with the gradual increase in  $p\text{CO}_2$  over the next 100 years. A reduction in DMS concentration will affect the atmospheric flux of sulfur from the marine environment. As many of these mesocosm experiments have been performed in a single location in Norway, further large-scale mesocosm experiments should be performed in different oceanic regions, to assess the changes in the parameters measured here for different microbial communities. Further investigations should concentrate on rates of DMSP production and the bacterial consumption of DMS and DMSP to develop a better

understanding of the interactions with the microbial community that affect the concentrations of these compounds. DMS and DMSP analyses should also be included in long-term (500+ generations) algal culture experiments, to establish if the short-term changes identified here are retained over a longer study period.

## Acknowledgements

The Bergen 2011 mesocosm experiment was part of the SOPRAN (Surface Ocean Processes in the Anthropocene; 03F0611C) 2 Programme funded by the German Ministry for Education and Research (BMBF) and led by the GEOMAR Helmholtz Centre for Ocean Research Kiel, Germany. The authors thank all participants in the SOPRAN Bergen experiment for their assistance. Special thanks to A. Ludwig for logistical support, J. Czerny, L. Bach and M. Meyerhöfer for discussions of the trace gas data and J. R. Bermudez for analysis of samples by light microscopy. The staff at the Espeyrend Marine Biological Station in Bergen, Norway, are acknowledged for their logistical support, in particular A. Aadnesen. The authors also thank R. Utting and A. Dimond for the support in the laboratory at the University of East Anglia. This work was funded by a UK Natural Environment Research Council Directed Research Studentship (NE/H025588/1) through the UK Ocean Acidification Research Programme, with CASE funding from Plymouth Marine Laboratory. Additional funding was provided by the MINOS project funded by EU-ERC (project number 250254). The authors thank the three anonymous reviewers for their comments on improving this manuscript.

## References

- [1] D. L. Hartmann, A. M. G. Klein Tank, M. Rusticucci, L. V. Alexander, S. Bronnimann, Y. Charabi, Observations: atmosphere and surface, in *Climate Change 2013: The Physical Science Basis. Contribution of Working Group 1 to the Fifth Assessment Report of the Intergovernmental Panel on Climate Change* (Eds T.F. Stocker, D. Qin, G.-K. Plattner, M. Tignor, S.K. Allen, J. Boschung, A. Nauels, Y. Xia, V. Bex, P. M. Midgley) **2013** pp. 159–254 (Cambridge University Press: Cambridge, UK).
- [2] U. Cubasch, D. Wuebbles, D. Chen, M. C. Facchini, D. Frame, N. Mahowald, J.-Winther, G. Introduction, in *Climate Change 2013: The Physical Science Basis. Contribution of Working Group 1 to the Fifth Assessment Report of the Intergovernmental Panel on Climate Change* (Eds T. Stocker, D. Qin, G.-K. Plattner, M. Tignor, S. K. Allen, J. Boschung, A. Nauels, Y. Xia, V. Bex, P. M. Midgley) **2013**, pp. 119–158 (Cambridge University Press: Cambridge, UK).
- [3] C. Le Quéré, G. P. Peters, R. J. Andres, R. M. Andrew, T. A. Boden, P. Ciais, P. Friedlingstein, R. A. Houghton, G. Marland, R. Moriarty, S. Sitch, P. Tans, A. Arneeth, A. Arvanitis, D. C. E. Bakker, L. Bopp, J. G. Canadell, L. P. Chini, S. C. Doney, A. Harper, I. Harris, J. I. House, A. K. Jain, S. D. Jones, E. Kato, R. F. Keeling, K. Klein Goldewijk, A. Körtzinger, C. Koven, N. Lefèvre, F. Maignan, A. Omar, T. Ono, G.-H. Park, B. Pfeil, B. Poulter, M. R. Raupach, P. Regnier, C. Rödenbeck, S. Saito, J. Schwinger, J. Segsneider, B. D. Stocker, T. Takahashi, B. Tilbrook, S. van Heuven, N. Viovy, R. Wanninkhof, A. Wiltshire, S. Zaehle, Global carbon budget 2013. *Earth Syst. Sci. Data* **2014**, *6*, 235. doi:10.5194/ESSD-6-235-2014
- [4] R. A. Feely, S. C. Doney, S. R. Cooley, Ocean acidification: present conditions and future changes in a high  $\text{CO}_2$  world. *Oceanography* **2009**, *22*, 36. doi:10.5670/OCEANOGRAPHY.2009.95
- [5] J. C. Orr, V. J. Fabry, O. Aumont, L. Bopp, S. C. Doney, R. A. Feely, A. Gnanadesikan, N. Gruber, A. Ishida, F. Joos, R. M. Key, K. Lindsay, E. Maier-Reimer, R. Matear, P. Monfray, A. Mouchet, R. G. Najjar, G.-K. Plattner, K. B. Rodgers, C. L. Sabine, J. L. Sarmiento, R. Schlitzer, R. D. Slater, I. J. Totterdell, M.-F. Weirig, Y. Yamanaka, A. Yool, Anthropogenic ocean acidification over the twenty-first century and its impact on calcifying organisms. *Nature* **2005**, *437*, 681. doi:10.1038/NATURE04095
- [6] P. M. Holligan, M. Viollier, D. S. Harbour, P. Camus, M. Champagne-Phillipe, Satellite and ship studies of coccolithophore production along

- a continental shelf edge. *Nature* **1983**, *304*, 339. doi:10.1038/304339A0
- [7] P. M. Holligan, E. Fernandez, J. Aiken, W. M. Balch, P. Boyd, P. H. Burkhill, M. Finch, S. B. Groom, G. Malin, K. Muller, D. A. Purdie, C. C. Trees, C. Robinson, S. M. Turner, P. van der Wal, A biogeochemical study of the coccolithophore *Emiliana huxleyi* in the North Atlantic. *Global Biogeochem. Cycles* **1993**, *7*, 879. doi:10.1029/93GB01731
- [8] U. Riebesell, I. Zondervan, B. Rost, P. D. Tortell, R. E. Zeebe, F. M. M. Morel, Reduced calcification of marine plankton in response to increased atmospheric CO<sub>2</sub>. *Nature* **2000**, *407*, 364. doi:10.1038/35030078
- [9] A. Sciandra, J. Harlay, D. Lefèvre, R. Lemée, P. Rimmelin, M. Denis, J.-P. Gattuso, Response of coccolithophorid *Emiliana huxleyi* to elevated partial pressure of CO<sub>2</sub> under nitrogen limitation. *Mar. Ecol. Prog. Ser.* **2003**, *261*, 111. doi:10.3354/MEPS261111
- [10] I. Zondervan, R. E. Zeebe, B. Rost, U. Riebesell, Decreasing marine biogenic calcification: a negative feedback on rising pCO<sub>2</sub>. *Global Biogeochem. Cycles* **2001**, *15*, 507. doi:10.1029/2000GB001321
- [11] H. Elderfield, Carbonate mysteries. *Science* **2002**, *296*, 1618. doi:10.1126/SCIENCE.1072079
- [12] A. Vairavamurthy, M. O. Andreae, R. L. Iverson, Biosynthesis of dimethylsulfide and dimethylpropiothetin by *Hymenomonas carterae* in relation to sulfur source and salinity variations. *Limnol. Oceanogr.* **1985**, *30*, 59. doi:10.4319/LO.1985.30.1.0059
- [13] M. Levasseur, Impact of Arctic meltdown on microbial cycling of sulphur. *Nat. Geosci.* **2013**, *6*, 691. doi:10.1038/NGEO1910
- [14] W. Sunda, D. J. Kieber, R. P. Kiene, S. Huntsman, An antioxidant function for DMSP and DMS in marine algae. *Nature* **2002**, *418*, 317. doi:10.1038/NATURE00851
- [15] S. Strom, G. Wolfe, J. Holmes, H. Stecher, C. Shimeneck, S. Lambert, E. Moreno, Chemical defense in the microplankton I: Feeding and growth rates of heterotrophic protists on the DMS-producing phytoplankton *Emiliana huxleyi*. *Limnol. Oceanogr.* **2003**, *48*, 217. doi:10.4319/LO.2003.48.1.0217
- [16] J. R. Seymour, R. Simó, T. Ahmed, R. Stocker, Chemoattraction to dimethylsulfoniopropionate throughout the marine microbial food web. *Science* **2010**, *329*, 342. doi:10.1126/SCIENCE.1188418
- [17] M. Garren, K. Son, J.-B. Raina, R. Rusconi, F. Menolascina, O. H. Shapiro, J. Tout, D. G. Bourne, J. R. Seymour, R. Stocker, A bacterial pathogen uses dimethylsulfoniopropionate as a cue to target heat-stressed corals. *ISME J.* **2014**, *8*, 999. doi:10.1038/ISMEJ.2013.210
- [18] R. Simó, M. Vila-Costa, L. Alonso-Sáez, C. Cardelús, Ó. Guadayol, E. Vázquez-Domínguez, J. M. Gasol, Annual DMSP contribution to S and C fluxes through phytoplankton and bacterioplankton in a NW Mediterranean coastal site. *Aquat. Microb. Ecol.* **2009**, *57*, 43. doi:10.3354/AME01325
- [19] M. Vila-Costa, R. Simó, H. Harada, J. M. Gasol, D. Slezak, R. P. Kiene, Dimethylsulfoniopropionate uptake by marine phytoplankton. *Science* **2006**, *314*, 652. doi:10.1126/SCIENCE.1131043
- [20] R. J. Charlson, J. E. Lovelock, M. O. Andreae, S. G. Warren, Oceanic phytoplankton, atmospheric sulfur, cloud albedo and climate. *Nature* **1987**, *326*, 655. doi:10.1038/326655A0
- [21] P. K. Quinn, T. S. Bates, The case against climate regulation via oceanic phytoplankton sulphur emissions. *Nature* **2011**, *480*, 51. doi:10.1038/NATURE10580
- [22] A. Lana, T. G. Bell, R. Simó, S. M. Vallina, J. Ballabrera-Poy, A. J. Kettle, J. Dachs, L. Bopp, E. S. Saltzman, J. Stefels, J. E. Johnson, P. S. Liss, An updated climatology of surface dimethylsulfide concentrations and emission fluxes in the global ocean. *Global Biogeochem. Cycles* **2011**, *25*, GB1004. doi:10.1029/2010GB003850
- [23] S. D. Archer, S. A. Kimmance, J. A. Stephens, F. E. Hopkins, R. G. J. Bellerby, K. G. Schulz, J. Piontek, A. Engel, Contrasting responses of DMS and DMSP to ocean acidification in Arctic waters. *Biogeosciences* **2013**, *10*, 1893. doi:10.5194/BG-10-1893-2013
- [24] F. E. Hopkins, S. M. Turner, P. D. Nightingale, M. Steinke, D. Bakker, P. S. Liss, Ocean acidification and marine trace gas emissions. *Proc. Natl. Acad. Sci. USA* **2010**, *107*, 760. doi:10.1073/PNAS.0907163107
- [25] V. Avgoustidi, P. D. Nightingale, I. Joint, M. Steinke, S. M. Turner, F. E. Hopkins, Decreased marine dimethyl sulfide production under elevated CO<sub>2</sub> levels in mesocosm and in vitro studies. *Environ. Chem.* **2012**, *9*, 399. doi:10.1071/EN11125
- [26] J.-M. Kim, K. Lee, E. J. Yang, K. Shin, J. H. Noh, K.-T. Park, B. Hyun, H.-J. Jeong, J.-H. Kim, K. Y. Kim, M. Kim, H.-C. Kim, P.-G. Jang, M.-C. Jang, Enhanced production of oceanic dimethylsulfide resulting from CO<sub>2</sub>-induced grazing activity in a high CO<sub>2</sub> world. *Environ. Sci. Technol.* **2010**, *44*, 8140. doi:10.1021/ES102028K
- [27] K.-T. Park, K. Lee, K. Shin, E. J. Yang, B. Hyun, J.-M. Kim, J. H. Noh, M. Kim, B. Kong, D. H. Choi, S.-J. Choi, P.-G. Jang, H. J. Jeong, Direct linkage between dimethyl sulfide production and microzooplankton grazing, resulting from prey composition change under high partial pressure of carbon dioxide conditions. *Environ. Sci. Technol.* **2014**, *48*, 4750. doi:10.1021/ES403351H
- [28] M. Vogt, M. Steinke, S. M. Turner, A. Paulino, M. Meyerhöfer, U. Riebesell, C. LeQuéré, P. S. Liss, Dynamics of dimethylsulphoniopropionate and dimethylsulphide under different CO<sub>2</sub> concentrations during a mesocosm experiment. *Biogeosciences* **2008**, *5*, 407. doi:10.5194/BG-5-407-2008
- [29] F. E. Hopkins, S. D. Archer, Consistent increase in dimethyl sulphide (DMS) in response to high CO<sub>2</sub> in five shipboard bioassays from contrasting NW European waters. *Biogeosciences* **2014**, *11*, 4925. doi:10.5194/BG-11-4925-2014
- [30] J. Piontek, C. Borchard, M. Sperling, K. G. Schulz, U. Riebesell, A. Engel, Response of bacterioplankton activity in an Arctic fjord system to elevated pCO<sub>2</sub>: results from a mesocosm perturbation study. *Biogeosciences* **2013**, *10*, 297. doi:10.5194/BG-10-297-2013
- [31] S. Endres, L. Galgani, U. Riebesell, K.-G. Schulz, A. Engel, Stimulated bacterial growth under elevated pCO<sub>2</sub>: results from an off-shore mesocosm study. *PLoS One* **2014**, *9*, e99228. doi:10.1371/JOURNAL.PONE.0099228
- [32] R. A. Andersen, J. A. Berges, P. J. Harrison, M. M. Watanabe, *Algal Culturing Techniques*. **2005** (Imprint Academic Press: London).
- [33] N. Jaeckisch, I. Yang, S. Wohrab, G. Glöckner, J. Kroymann, H. Vogel, A. Cembella, U. John, Comparative genomic and transcriptomic characterization of the toxigenic marine dinoflagellate *Alexandrium ostenfeldii*. *PLoS One* **2011**, *6*, e28012. doi:10.1371/JOURNAL.PONE.0028012
- [34] A. G. Dickson, The measurement of sea water pH. *Mar. Chem.* **1993**, *44*, 131. doi:10.1016/0304-4203(93)90198-W
- [35] A. G. Dickson, The carbon dioxide system in seawater: equilibrium chemistry and measurements, in *Guide to Best Practices for Ocean Acidification Research and Data Reporting* (Eds U. Riebesell, V. J. Fabry, L. Hansson, J.-P. Gattuso) **2010**, pp. 17–40 (Publications Office of the European Union: Luxembourg).
- [36] *Proficiency Study 12–23: DMS in Seawater* **2013** (National Measurement Institute of Australia).
- [37] U. Riebesell, J. Czerny, K. von Bröckel, T. Boxhammer, J. Büdenbender, M. Deckelnick, M. Fischer, D. Hoffmann, S. A. Krug, U. Lentz, A. Ludwig, R. Mücke, K. G. Schulz, Technical Note: a mobile sea-going mesocosm system – new opportunities for ocean change research. *Biogeosciences* **2013**, *10*, 1835. doi:10.5194/BG-10-1835-2013
- [38] K. G. Schulz, J. Barcelos e Ramos, R. E. Zeebe, U. Riebesell, CO<sub>2</sub> perturbation experiments: similarities and differences between dissolved inorganic carbon and total alkalinity manipulations. *Biogeosciences* **2009**, *6*, 2145. doi:10.5194/BG-6-2145-2009
- [39] K. Johnson, J. M. Sieburth, P. J. le B. Williams, L. Brändström, Coulometric total carbon dioxide analysis for marine studies: automation and calibration. *Mar. Chem.* **1987**, *21*, 117. doi:10.1016/0304-4203(87)90033-8
- [40] A. G. Dickson, C. L. Sabine, J. R. Christian, (Eds) *Guide to Best Practices for Ocean CO<sub>2</sub> Measurements*. *PICES Special Publication 3* **2007** (Carbon Dioxide Information Analysis Center: Oak Ridge,

- TN, USA). Available at [http://cdiac.ornl.gov/oceans/Handbook\\_2007.html](http://cdiac.ornl.gov/oceans/Handbook_2007.html) [Verified 29 August 2015].
- [41] C. Mehrbach, C. H. Culbertson, J. E. Hawley, R. M. Pytkowicz, Measurement of the apparent dissociation constants of carbonic acid in seawater at atmospheric pressure. *Limnol. Oceanogr.* **1973**, *18*, 897. doi:10.4319/LO.1973.18.6.0897
- [42] T. J. Lueker, A. G. Dickson, C. D. Keeling, Ocean  $p\text{CO}_2$  calculated from dissolved inorganic carbon, alkalinity, and equations for K1 and K2: validation based on laboratory measurements of  $\text{CO}_2$  in gas and seawater at equilibrium. *Mar. Chem.* **2000**, *70*, 105. doi:10.1016/S0304-4203(00)00022-0
- [43] A. L. Chuck, S. M. Turner, P. S. Liss, Oceanic distributions and air-sea fluxes of biogenic halocarbons in the open ocean. *J. Geophys. Res.* **2005**, *110*, C10022. doi:10.1029/2004JC002741
- [44] C. Hughes, G. Malin, P. D. Nightingale, P. S. Liss, The effect of light stress on the release of volatile iodocarbons by three species of marine microalgae. *Limnol. Oceanogr.* **2006**, *51*, 2849. doi:10.4319/LO.2006.51.6.2849
- [45] M. Martino, P. S. Liss, J. M. C. Plane, The photolysis of dihalomethanes in surface seawater. *Environ. Sci. Technol.* **2005**, *39*, 7097. doi:10.1021/ES048718S
- [46] M. A. J. Curran, G. B. Jones, H. Burton, Spatial distribution of dimethylsulfide and dimethylsulfoniopropionate in the Australasian sector of the Southern Ocean. *J. Geophys. Res.* **1998**, *103*, 16 677. doi:10.1029/97JD03453
- [47] R. P. Kiene, D. Slezak, Low dissolved DMSP concentrations in seawater revealed by small-volume gravity filtration and dialysis sampling. *Limnol. Oceanogr. Methods* **2006**, *4*, 80. doi:10.4319/LOM.2006.4.80
- [48] A. Larsen, T. Castberg, R. A. Sandaa, C. P. D. Brussaard, J. Egge, M. Heldal, A. Paulino, R. Thyraug, E. J. van Hannen, G. Bratbak, Population dynamics and diversity of phytoplankton, bacteria and viruses in a seawater enclosure. *Mar. Ecol. Prog. Ser.* **2001**, *221*, 47. doi:10.3354/MEPS221047
- [49] N. A. Welschmeyer, Fluorometric analysis of chlorophyll-*a* in the presence of chlorophyll-*b* and pheopigments. *Limnol. Oceanogr.* **1994**, *39*, 1985. doi:10.4319/LO.1994.39.8.1985
- [50] R. G. Barlow, D. G. Cummings, S. W. Gibb, Improved resolution of mono- and divinyl chlorophylls a and b and zeaxanthin and lutein in phytoplankton extracts using reverse phase C-8 HPLC. *Mar. Ecol. Prog. Ser.* **1997**, *161*, 303. doi:10.3354/MEPS161303
- [51] M. D. Mackey, D. J. Mackey, H. W. Higgins, S. W. Wright, CHEMTAX a program for estimating class abundances from chemical markers: application to HPLC measurements of phytoplankton. *Mar. Ecol. Prog. Ser.* **1996**, *144*, 265. doi:10.3354/MEPS144265
- [52] K. G. Schulz, R. G. J. Bellerby, C. P. D. Brussaard, J. Bűdenbender, J. Czerny, A. Engel, M. Fischer, S. Koch-Klavsen, S. A. Krug, S. Lischka, A. Ludwig, M. Meyerhűfer, G. Nondal, A. Silyakova, A. Stuhr, U. Riebesell, Temporal biomass dynamics of an Arctic plankton bloom in response to increasing levels of atmospheric carbon dioxide. *Biogeosciences* **2013**, *10*, 161. doi:10.5194/BG-10-161-2013
- [53] M. Steinke, C. Evans, G. A. Lee, G. Malin, Substrate kinetics of DMSP-lyases in axenic cultures and mesocosm populations of *Emiliania huxleyi*. *Aquat. Sci.* **2007**, *69*, 352. doi:10.1007/S00027-007-0893-2
- [54] M. Levasseur, S. Michaud, J. Egge, G. Cantin, J. C. Nejtgaard, R. Sanders, E. Fernandez, P. T. Solberg, B. Heimdal, M. Gosselin, Production of DMSP and DMS during a mesocosm study of an *Emiliania huxleyi* bloom: influence of bacteria and *Calanus finmarchicus* grazing. *Mar. Biol.* **1996**, *126*, 609. doi:10.1007/BF00351328
- [55] M. Hein, K. Sand-Jensen,  $\text{CO}_2$  increases oceanic primary production. *Nature* **1997**, *388*, 526. doi:10.1038/41457
- [56] B. Rost, U. Riebesell, S. Burkhardt, D. Sultemeyer, Carbon acquisition of bloom-forming marine phytoplankton. *Limnol. Oceanogr.* **2003**, *48*, 55. doi:10.4319/LO.2003.48.1.0055
- [57] B. Rost, I. Zondervan, D. Wolf-Gladrow, Sensitivity of phytoplankton to future changes in ocean carbonate chemistry: current knowledge, contradictions and research directions. *Mar. Ecol. Prog. Ser.* **2008**, *373*, 227. doi:10.3354/MEPS07776
- [58] C. P. D. Brussaard, A. A. M. Noordeloos, H. Witte, M. C. J. Collenteur, K. Schulz, A. Ludwig, U. Riebesell, Arctic microbial community dynamics influenced by elevated  $\text{CO}_2$  levels. *Biogeosciences* **2013**, *10*, 719. doi:10.5194/BG-10-719-2013
- [59] Y. Wu, D. A. Campbell, A. J. Irwin, D. J. Suggett, Z. V. Finkel, Ocean acidification enhances the growth rate of larger diatoms. *Limnol. Oceanogr.* **2014**, *59*, 1027. doi:10.4319/LO.2014.59.3.1027
- [60] B. Delille, J. Harlay, I. Zondervan, S. Jacquet, L. Chou, R. Wollast, R. G. J. Bellerby, M. Frankignoulle, A. V. Borges, U. Riebesell, J.-P. Gattuso, Response of primary production and calcification to changes of  $p\text{CO}_2$  during experimental blooms of the coccolithophorid *Emiliania huxleyi*. *Global Biogeochem. Cycles* **2005**, *19*, GB2023. doi:10.1029/2004GB002318
- [61] B. S. C. Leadbeater, Identification, by means of electron microscopy, of flagellate nanoplankton from the coast of Norway. *Sarsia* **1972**, *49*, 107.
- [62] S. Jacquet, M. Heldal, M. D. Iglesias-Rodríguez, A. Larsen, W. Wilson, G. Bratbak, Flow cytometric analysis of an *Emiliania huxleyi* bloom terminated by viral infection. *Aquat. Microb. Ecol.* **2002**, *27*, 111. doi:10.3354/AME027111
- [63] M. J. Frada, K. D. Bidle, I. Probert, C. de Vargas, In situ survey of life cycle phases of the coccolithophore *Emiliania huxleyi* (Haptophyta). *Environ. Microbiol.* **2012**, *14*, 1558. doi:10.1111/J.1462-2920.2012.02745.X
- [64] Y. Feng, C. E. Hare, K. Leblanc, J. M. Rose, Y. Zhang, G. R. DiTullio, P. A. Lee, S. W. Wilhelm, J. M. Rowe, J. Sun, N. Nemcek, C. Gueguen, U. Passow, I. Benner, C. Brown, D. A. Hutchins, Effects of increased  $p\text{CO}_2$  and temperature on the North Atlantic spring bloom. I. The phytoplankton community and biogeochemical response. *Mar. Ecol. Prog. Ser.* **2009**, *388*, 13. doi:10.3354/MEPS08133
- [65] A. Spielmeyer, G. Pohnert, Influence of temperature and elevated carbon dioxide on the production of dimethylsulfoniopropionate and glycine betaine by marine phytoplankton. *Mar. Environ. Res.* **2012**, *73*, 62.
- [66] G. Langer, G. Nehrke, I. Probert, J. Ly, P. Ziveri, Strain-specific responses of *Emiliania huxleyi* to changing seawater carbonate chemistry. *Biogeosciences* **2009**, *6*, 2637. doi:10.5194/BG-6-2637-2009
- [67] N. A. Nimer, M. J. Merrett, Calcification rate in *Emiliania huxleyi* Lohmann in response to light, nitrate and availability of inorganic carbon. *New Phytol.* **1993**, *123*, 673. doi:10.1111/J.1469-8137.1993.TB03776.X
- [68] K. T. Lohbeck, U. Riebesell, S. Collins, T. B. H. Reusch, Functional genetic divergence in high  $\text{CO}_2$  adapted *Emiliania huxleyi* populations. *Evolution* **2013**, *67*, 1892. doi:10.1111/J.1558-5646.2012.01812.X
- [69] H. E. Arnold, P. Kerrison, M. Steinke, Interacting effects of ocean acidification and warming on growth and DMS-production in the haptophyte coccolithophore *Emiliania huxleyi*. *Glob. Change Biol.* **2013**, *19*, 1007. doi:10.1111/GCB.12105
- [70] D. Shi, Y. Xu, F. M. M. Morel, Effects of the pH/ $p\text{CO}_2$  control method on medium chemistry and phytoplankton growth. *Biogeosciences* **2009**, *6*, 1199. doi:10.5194/BG-6-1199-2009
- [71] N. A. Nimer, M. J. Merrett, Calcification and utilization of inorganic carbon by the coccolithophorid *Emiliania huxleyi* Lohmann. *New Phytol.* **1992**, *121*, 173. doi:10.1111/J.1469-8137.1992.TB01102.X
- [72] A. Engel, I. Zondervan, K. Aerts, L. Beaufort, A. Benthien, L. Chou, B. Delille, J.-P. Gattuso, J. Harlay, C. Heemann, L. Hoffmann, S. Jacquet, J. C. Nejtgaard, M.-D. Pizay, E. Rochelle-Newall, U. Schneider, A. Terbrueggen, U. Riebesell, Testing the direct effect of  $\text{CO}_2$  concentration on a bloom of the coccolithophorid *Emiliania huxleyi* in mesocosm experiments. *Limnol. Oceanogr.* **2005**, *50*, 493. doi:10.4319/LO.2005.50.2.0493
- [73] L. F. Dong, N. A. Nimer, E. Okus, M. J. Merrett, Dissolved inorganic carbon utilization in relation to calcite production in *Emiliania huxleyi* (Lohmann) Kamptner. *New Phytol.* **1993**, *123*, 679. doi:10.1111/J.1469-8137.1993.TB03777.X

- [74] D. M. Kottmeier, S. D. Rokitta, P. D. Tortell, B. Rost, Strong shift from HCO<sub>3</sub> to CO<sub>2</sub> uptake in *Emiliania huxleyi* with acidification: new approach unravels acclimation versus short-term pH effects. *Photosynth. Res.* **2014**, *121*, 265. doi:10.1007/S11120-014-9984-9
- [75] M. D. Iglesias-Rodriguez, P. R. Halloran, R. E. M. Rickaby, I. R. Hall, E. Colmenero-Hidalgo, J. R. Gittins, D. R. H. Green, T. Tyrrell, S. J. Gibbs, P. von Dassow, E. Rehm, E. V. Armbrust, K. P. Boessenkool, Phytoplankton calcification in a high-CO<sub>2</sub> world. *Science* **2008**, *320*, 336. doi:10.1126/SCIENCE.1154122
- [76] J. Barcelos e Ramos, M. N. Müller, U. Riebesell, Short-term response of the coccolithophore *Emiliania huxleyi* to an abrupt change in seawater carbon dioxide concentrations. *Biogeosciences* **2010**, *7*, 177. doi:10.5194/BG-7-177-2010
- [77] M. Heinle, *The effects of light, temperature and nutrients on coccolithophores and implications for biogeochemical models* **2013**, Ph.D. thesis, University of East Anglia, Norwich, UK.
- [78] P. W. Boyd, T. A. Rynearson, E. A. Armstrong, F. Fu, K. Hayashi, Z. Hu, D. A. Hutchins, R. M. Kudela, E. Litchman, M. R. Mulholland, U. Passow, R. F. Strzeppek, K. A. Whittaker, E. Yu, M. K. Thomas, Marine phytoplankton temperature versus growth responses from polar to tropical waters – outcome of a scientific community-wide study. *PLoS One* **2013**, *8*, e63091. doi:10.1371/JOURNAL.PONE.0063091
- [79] M. N. Müller, K. G. Schulz, U. Riebesell, Effects of long-term high CO<sub>2</sub> exposure on two species of coccolithophores. *Biogeosciences* **2010**, *7*, 1109. doi:10.5194/BG-7-1109-2010
- [80] K. T. Lohbeck, U. Riebesell, T. B. H. Reusch, Adaptive evolution of a key phytoplankton species to ocean acidification. *Nat. Geosci.* **2012**, *5*, 346. doi:10.1038/NNGEO1441
- [81] D. J. Franklin, M. Steinke, J. Young, I. Probert, G. Malin, Dimethylsulphoniopropionate (DMSP), DMSP-lyase activity (DLA) and dimethylsulfide (DMS) in 10 species of coccolithophore. *Mar. Ecol. Prog. Ser.* **2010**, *410*, 13. doi:10.3354/MEPS08596
- [82] J. C. Cubillos, S. W. Wright, G. Nash, M. F. de Salas, B. Griffiths, B. Tilbrook, A. Poisson, G. M. Hallegraeff, Calcification morphotypes of the coccolithophorid *Emiliania huxleyi* in the Southern Ocean: changes in 2001 to 2006 compared to historical data. *Mar. Ecol. Prog. Ser.* **2007**, *348*, 47. doi:10.3354/MEPS07058
- [83] A. Winter, J. Henderiks, L. Beaufort, R. E. M. Rickaby, C. W. Brown, Poleward expansion of the coccolithophore *Emiliania huxleyi*. *J. Plankton Res.* **2014**, *36*, 316. doi:10.1093/PLANKT/FBT110
- [84] T. Wuori, *The effects of elevated pCO<sub>2</sub> in the physiology of Emiliania huxleyi* **2012**, M.Sc. Thesis, Western Washington University, Bellingham, WA, USA.
- [85] M. G. Scarratt, M. Levasseur, S. Michaud, S. Roy, DMSP and DMS in the Northwest Atlantic: late-summer distributions, production rates and sea-air fluxes. *Aquat. Sci.* **2007**, *69*, 292. doi:10.1007/S00027-007-0886-1
- [86] C. Leck, U. Larsson, L. E. Bågander, S. Johansson, S. Hajdu, Dimethyl sulfide in the Baltic Sea: annual variability in relation to biological activity. *J. Geophys. Res.* **1990**, *95*, 3353. doi:10.1029/JC095IC03P03353
- [87] S. M. Turner, G. Malin, P. S. Liss, D. S. Harbour, P. M. Holligan, The seasonal variation of dimethyl sulfide and dimethylsulfonylpropionate concentrations in nearshore waters. *Limnol. Oceanogr.* **1988**, *33*, 364. doi:10.4319/LO.1988.33.3.0364
- [88] A. Lana, R. Simó, S. M. Vallina, J. Dachs, Re-examination of global emerging patterns of ocean DMS concentration. *Biogeochemistry* **2012**, *110*, 173. doi:10.1007/S10533-011-9677-9
- [89] P. S. Liss, A. D. Hatton, G. Malin, P. D. Nightingale, S. M. Turner, Marine sulphur emissions. *Philos. Trans. R. Soc. B Biol. Sci.* **1997**, *352*, 159. doi:10.1098/RSTB.1997.0011
- [90] M. Galí, R. Simó, A meta-analysis of oceanic DMS and DMSP cycling processes: disentangling the summer paradox. *Global Biogeochem. Cycles* **2015**, *29*, 496. doi:10.1002/2014GB004940
- [91] R. Simó, C. Pedrós-Alió, Role of vertical mixing in controlling the oceanic production of dimethyl sulphide. *Nature* **1999**, *402*, 396. doi:10.1038/46516
- [92] A. R. J. Curson, J. D. Todd, M. J. Sullivan, A. W. B. Johnston, Catabolism of dimethylsulphonylpropionate: microorganisms, enzymes and genes. *Nat. Rev. Microbiol.* **2011**, *9*, 849. doi:10.1038/NRMICRO2653
- [93] E. C. Howard, J. R. Henriksen, A. Buchan, C. R. Reisch, H. Bürgmann, R. Welsh, W. Ye, J. M. González, K. Mace, S. B. Joye, R. P. Kiene, W. B. Whitman, M. A. Moran, Bacterial taxa that limit sulphur flux from the ocean. *Science* **2006**, *314*, 649. doi:10.1126/SCIENCE.1130657
- [94] J. D. Todd, R. Rogers, Y. G. Li, M. Wexler, P. L. Bond, L. Sun, A. R. J. Curson, G. Malin, M. Steinke, A. W. B. Johnston, Structural and regulatory genes required to make the gas dimethyl sulfide in bacteria. *Science* **2007**, *315*, 666. doi:10.1126/SCIENCE.1135370
- [95] E. C. Howard, S. Sun, C. R. Reisch, D. A. del Valle, H. Bürgmann, R. P. Kiene, M. A. Moran, Changes in dimethylsulfonylpropionate demethylase gene assemblages in response to an induced phytoplankton bloom. *Appl. Environ. Microbiol.* **2011**, *77*, 524. doi:10.1128/AEM.01457-10
- [96] M. Zubkov, L. J. Linn, R. Amann, R. P. Kiene, Temporal patterns of biological dimethylsulfide (DMS) consumption during laboratory-induced phytoplankton bloom cycles. *Mar. Ecol. Prog. Ser.* **2004**, *271*, 77. doi:10.3354/MEPS271077
- [97] B. R. Mohapatra, A. N. Rellinger, D. J. Kieber, R. P. Kiene, Kinetics of DMSP lyases in whole cell extracts of four *Phaeocystis* species: response to temperature and DMSP analogs. *J. Sea Res.* **2014**, *86*, 110. doi:10.1016/J.SEARES.2013.11.012
- [98] C.-Y. Li, T.-D. Wei, S.-H. Zhang, X.-L. Chen, X. Gao, P. Wang, B.-B. Xie, H.-N. Su, Q.-L. Qin, X.-Y. Zhang, J. Yu, H.-H. Zhang, B.-C. Zhou, G.-P. Yang, Y.-Z.-Zhang, Molecular insight into bacterial cleavage of oceanic dimethylsulfonylpropionate into dimethyl sulfide. *Proc. Natl. Acad. Sci. USA* **2014**, *111*, 1026. doi:10.1073/PNAS.1312354111
- [99] M. De Souza, D. Yoch, Comparative physiology of dimethyl sulfide production by dimethylsulfonylpropionate lyase in *Pseudomonas doudoroffii* and *Alcaligenes* sp. strain M3A. *Appl. Environ. Microbiol.* **1995**, *61*, 3986.
- [100] J. Stefels, L. Dijkhuizen, Characteristics of DMSP-lyase in *Phaeocystis* sp. (Prymnesiophyceae). *Mar. Ecol. Prog. Ser.* **1996**, *131*, 307. doi:10.3354/MEPS131307
- [101] R. P. Kiene, L. J. Linn, J. A. Bruton, New and important roles for DMSP in marine microbial communities. *J. Sea Res.* **2000**, *43*, 209. doi:10.1016/S1385-1101(00)00023-X
- [102] M. Vila-Costa, D. A. del Valle, J. M. González, D. Slezak, R. P. Kiene, O. Sánchez, R. Simó, Phylogenetic identification and metabolism of marine dimethylsulfide-consuming bacteria. *Environ. Microbiol.* **2006**, *8*, 2189. doi:10.1111/J.1462-2920.2006.01102.X
- [103] H. Schäfer, Isolation of *Methylophaga* spp. from marine dimethylsulfide-degrading enrichment cultures and identification of polypeptides induced during growth on dimethylsulfide. *Appl. Environ. Microbiol.* **2007**, *73*, 2580. doi:10.1128/AEM.02074-06
- [104] R. P. Kiene, D. M. Shenoy, M. C. Hart, A. Mogg, D. H. Green, Metabolism of DMSP, DMS and DMSO by the cultivable bacterial community associated with the DMSP-producing dinoflagellate *Scrippsiella trochoidea*. *Biogeochemistry* **2012**, *110*, 131. doi:10.1007/S10533-012-9702-7
- [105] J. Pinhassi, R. Simó, J. M. González, M. Vila, L. Alonso-Saez, R. P. Kiene, M. A. Moran, C. Pedros-Alió, Dimethylsulfonylpropionate turnover is linked to the composition and dynamics of the bacterioplankton assemblage during a microcosm phytoplankton bloom. *Appl. Environ. Microbiol.* **2005**, *71*, 7650. doi:10.1128/AEM.71.12.7650-7660.2005
- [106] M. G. Scarratt, M. Levasseur, S. Schultes, S. Michaud, G. Cantin, A. Vezina, M. Gosselin, S. J. De Mora, Production and consumption of dimethylsulfide (DMS) in North Atlantic waters. *Mar. Ecol. Prog. Ser.* **2000**, *204*, 13. doi:10.3354/MEPS204013